Possible role of electrodynamic interactions in long-distance biomolecular recognition

Jordane Preto,[1,2,3,*] Marco Pettini,[2,3,†] and Jack A. Tuszynski[4,5,‡]
[1]*Department of Chemistry, Rice University, Houston, Texas, USA*
[2]*Aix-Marseille University, Marseille, France*
[3]*CNRS Centre de Physique Théorique UMR7332, 13288 Marseille, France*
[4]*Department of Oncology, 3-336, Cross Cancer Institute, Edmonton, Alberta, Canada T6G 1Z2*
[5]*Department of Physics, University of Alberta, Edmonton, Alberta, Canada*
(Received 28 February 2014; revised manuscript received 31 August 2014; published 22 May 2015)

The issue of retarded long-range resonant interactions between two molecules with oscillating dipole moments is revisited within the framework of classical electrodynamics. By taking advantage of a theorem in complex analysis, we present a simple method to calculate the frequencies of the normal modes, which are then used to estimate the interaction potential. The possibility that such interactions play a non-negligible role in ensuring the effective functioning of the biomolecular functions is investigated. On the basis of experimental results reported in the literature and simple numerical estimates, it is found that long-range interactions involving electromagnetic fields of frequencies 0.1–1 THz could be temporarily activated despite radiation losses and solvent dissipation. Moreover, the theoretical background used to derive the mentioned interactions sheds light on Fröhlich's theory of selective long-range forces between biomolecules. At variance with a long-standing belief, we show that sizable resonant long-range interactions may exist only if the interacting system is out of thermal equilibrium.

DOI: 10.1103/PhysRevE.91.052710 PACS number(s): 87.10.−e, 34.20.Gj, 03.50.De, 12.20.−m

I. INTRODUCTION

For several decades now, understanding biomolecular dynamics and general mechanisms of protein-protein or protein-DNA recognition has become a diverse and fascinating topic which still generates much interest in the biophysics community. Not only does this area of research seem unavoidable to explain the characteristic synergy within most biological organisms but it can also be applied, e.g., to investigate the microscopic origin of infectious diseases as well as to the design of new drugs whose efficiency depends on how fast the synthesized proteins find their biological target [1]. When dealing with biomolecular recognition, it is suitable to distinguish between the phase during which (globular) proteins need to find their target while freely moving within the aqueous biological environment (three-dimensional diffusion) and the phase when the protein and its target, which have finally arrived in each other's vicinity, are in close contact. The latter is characterized by orientational and conformational adjustments of the biomolecules so that a biochemical reaction can eventually take place between them. At this stage, molecular motions are mainly governed by chemical forces of short-range nature (hydrophilic or hydrophobic interactions, van der Waals forces, covalent bonds, etc.) besides the traditional Brownian motion due to thermal fluctuations. Accurate information regarding the electrostatic charge distribution is needed to describe the dynamics and to estimate the associated rate constants. As far as the run-up to molecular encounter is concerned, the detailed topology of the molecules involved becomes irrelevant as the protein and its target are supposed to be far enough from one another. From a point of view of the dynamics, intermolecular electrostatic interactions might *a priori* play a role as those interactions are inherently of a long-range kind. However, cell cytoplasm contains considerable amounts of small ions which tend to screen any static electric charges at short range. The Debye length is typically smaller than 10 Å in cellular media. Even though the electrostatic field is screened at short distance, Debye screening turns out to be ineffective for electric fields oscillating at large enough frequencies. Oro showed experimentally that an electrolyte such as cell cytoplasm behaves like a pure dielectric (i.e., free of conducting properties) when acted upon by an electric field with frequencies larger than 250 MHz [2]. Such a threshold frequency was originally identified by Maxwell through analytical arguments in his *Treatise on Electricity and Magnetism* [3]. In any case, this suggests that electrodynamic intermolecular forces, i.e., forces between molecules carrying oscillating charges, might influence the encounter dynamics of biological cognate partners. Further theoretical investigations of these forces are required to probe their real contribution in a cellular environment.

Long-distance electrodynamic forces between two neutral atoms or small molecules have been broadly investigated in quantum electrodynamics (QED) [4]. Those forces typically arise when one of the atoms is in an excited state, and the transition frequencies of both atoms are similar. In quantum terms, this corresponds to the so-called exchange degeneracy which requires that the atoms remain in a quantum entangled state so that a net attraction (or repulsion) takes place [4]. Entangled states are very fragile, and, especially in a biological context, their existence over long distances could be questioned because of the noisy cellular environment. Thus, it is worth investigating long-distance interactions between biomolecules on a classical electrodynamics basis.

In the present paper, we show that, similarly to QED, attractive or repulsive long-distance electrodynamic interactions can be activated in conditions of classical resonance

*preto@cpt.univ-mrs.fr
†pettini@cpt.univ-mrs.fr
‡jack_BT@ualberta.ca

(see Sec. II). Off-resonance conditions lead to short-distance interactions. While quantum electrodynamic interactions are attributed to instantaneous dipole moments resulting from electronic transitions of the atoms, dipole moments involved in the classical limit are due to conformational molecular vibrations. Numerical estimates of resonant and nonresonant forces in a biological environment, taking into account the effects of radiation losses and solvent dissipation (viscosity, absorbance), are performed in Sec. III. We report possible physiological sources of energy that might trigger the mentioned forces and, by referring to recent experimental results—including terahertz detection of vibration modes of proteins, absorbance of biological tissues—we discuss why low-frequency electromagnetic signals can be momentarily sustained despite biological dissipation mechanisms. In such context, the water molecules surrounding the biomolecular structures should play an active role as suggested by recent experiments, especially to contribute and preserve dipolar protein vibrations. Due to the resonant nature of the forces, i.e., giving rise to long-range interactions only if the molecular structures involved vibrate at similar frequencies, attraction or repulsion between specific biological entities may exist thus creating order in a cellular environment over distances much larger than molecular dimensions.

In other words, there are reasons based on physical first principles to assign an essential role to an electromagnetic communication among biomolecules to account for the aforementioned highly efficient pattern of biochemical reactions in cells. This possibility has been hitherto overlooked, mainly because of two reasons. On the one hand, in the framework of short-range shape or dynamic complementarity (lock and key and induced fit) between cognate molecular partners, diffusion-driven random encounters between biomolecules seemed a natural and sufficient explanation. On the other hand, even though the idea of long-distance electromagnetic interactions between macromolecules has been sometimes surmised by physicists, the absence of any experimental strategy to convincingly detect their actual activation has marginalized this hypothesis. In this respect this work is motivated by the present day feasibility of experimental tests to assess whether such interactions could be relevant at the biomolecular level [5–7], hence the need for a thorough revisitation of the theoretical framework.

Based on apparently standard computations of classical electrodynamics, our present work resorts to a powerful inversion theorem in complex analysis and results in nontrivial development of a fascinating theory pioneered by Fröhlich [8–11] shedding light on some of its former results. In particular, we show that a commonly accepted result at thermal equilibrium is incorrect, that is, an electrodynamic interaction potential proportional to $-1/r^3$ (with r denoting the intermolecular distance) can be activated only out of thermal equilibrium. Moreover, additional interaction terms proportional to $-1/r^2$ and $-1/r$, both modulated in space, are found as field retardation effects; such terms are well known in QED, though the spatial modulation is still controversial, but in our classical framework these interaction terms are not associated with entanglement, as is the case with QED. A preliminary account of some of the results reported here was given in Ref. [12].

II. ELECTRODYNAMIC INTERACTIONS IN CLASSICAL PHYSICS

In order to assess whether electrodynamic interactions may play a sizable role in the organization of biomolecular reactions, in particular, by facilitating encounters of biomolecular cognate partners over long distances, the following sections are devoted to the investigation of classical electrodynamic interactions between two oscillating molecular dipoles. We focus on resonant properties of these interactions so that a particular biomolecule would be only attracted by its specific target, and not by other neighboring biomolecules. Field retardation effects are also taken into account.

A. Equations of motion

The far-field electrodynamic interactions between molecular systems mainly involve their dipole moments, that is, multipolar contributions can be neglected. Hence, we consider a simple system of two molecules A and B with dipole moments $\boldsymbol{\mu}_A$ and $\boldsymbol{\mu}_B$ oscillating with harmonic frequencies ω_A and ω_B, respectively. The corresponding equations of motion are written in the following general form:

$$\begin{aligned}\ddot{\boldsymbol{\mu}}_A + \gamma_A\dot{\boldsymbol{\mu}}_A + \omega_A^2\boldsymbol{\mu}_A &= \zeta_A\boldsymbol{E}_B(\boldsymbol{r}_A,t) + \boldsymbol{f}_A(\boldsymbol{\mu}_A,t)\\ \ddot{\boldsymbol{\mu}}_B + \gamma_B\dot{\boldsymbol{\mu}}_B + \omega_B^2\boldsymbol{\mu}_B &= \zeta_B\boldsymbol{E}_A(\boldsymbol{r}_B,t) + \boldsymbol{f}_B(\boldsymbol{\mu}_B,t).\end{aligned} \quad (1)$$

Since we have adopted the dipole approximation, the interaction between molecules is mediated by the electric field $\boldsymbol{E}_{A,B}(\boldsymbol{r},t)$ created by each dipole, here located at $\boldsymbol{r} = \boldsymbol{r}_{B,A}$. Related coupling constants are $\zeta_A = Q_A^2/m_A$, where Q_A and m_A are the effective charge and mass of dipole A, respectively, and ζ_B with a similar B-labeled expression. Other quantities are the damping coefficients $\gamma_{A,B}$ of the dipoles representing radiation losses, and functions $\boldsymbol{f}_{A,B}$ that describe, from a general point of view, possible anharmonic contributions of each dipole as well as possible external excitations.

Our goal here is to estimate the mean interaction energy of the system given by Eqs. (1). To proceed, we calculate its normal frequencies; starting from the associated harmonic conservative system:

$$\begin{aligned}\ddot{\boldsymbol{\mu}}_A + \omega_A^2\boldsymbol{\mu}_A &= \zeta_A\boldsymbol{E}_B(\boldsymbol{r}_A,t)\\ \ddot{\boldsymbol{\mu}}_B + \omega_B^2\boldsymbol{\mu}_B &= \zeta_B\boldsymbol{E}_A(\boldsymbol{r}_B,t)\end{aligned} \quad (2)$$

the normal frequencies are defined as the frequencies ω_N such that $\boldsymbol{\mu}_{A,B}(t) = \boldsymbol{\mu}_{A,B}e^{i\omega_N t}$ are solutions of Eqs. (2). In order to get ω_N, expressions of $\boldsymbol{E}_{A,B}(r,t)$ are computed explicitly. The computation of the electromagnetic field generated by an oscillating dipole is detailed in Appendix A. We assume that the dipole moment $\boldsymbol{\mu}$ in Eq. (A10) oscillates harmonically at frequency ω_N, i.e., $\boldsymbol{\mu} = \boldsymbol{\mu}_{A,B}\delta(\omega - \omega_N)$. Substituting this relation into Eq. (A10), we get after inverse Fourier transform

$$\boldsymbol{E}_B(\boldsymbol{r}_A,t) = \boldsymbol{\chi}(r,\omega_N)\boldsymbol{\mu}_B e^{i\omega_N t}, \quad (3)$$

where $r = |\boldsymbol{r}_A - \boldsymbol{r}_B|$ is the intermolecular distance; an analogous expression is given for $\boldsymbol{E}_A(\boldsymbol{r}_B,t)$. Here $\boldsymbol{\chi}(r,\omega)$ represents the susceptibility matrix of the electric field and is derived in

Appendix A [Eq. (A12)]. For $\omega \in \mathbb{C}$, one has

$$\chi_{11}(r,\omega) = \chi_{22}(r,\omega) = -\frac{e^{\pm i\omega\sqrt{\varepsilon(\omega)}r/c}}{\varepsilon(\omega)r^3} \times \left(1 \mp \frac{i\omega\sqrt{\varepsilon(\omega)}r}{c} - \frac{\omega^2\varepsilon(\omega)r^2}{c^2}\right), \quad (4a)$$

$$\chi_{33}(r,\omega) = \frac{2e^{\pm i\omega\sqrt{\varepsilon(\omega)}r/c}}{\varepsilon(\omega)r^3}\left(1 \mp \frac{i\omega\sqrt{\varepsilon(\omega)}r}{c}\right), \quad (4b)$$

with $\chi_{ij}(r,\omega) = 0$ when $i \neq j$; the $\pm$ sign is attributed to positive or negative values of $\mathrm{Im}(\omega\sqrt{\varepsilon(\omega)})$, respectively. We remark again that the diagonal form of $\boldsymbol{\chi}$ is due to the choice to set the z axis along r. For real values of ω_N, each element $\chi_{ii}(r,\omega_N)$ of $\boldsymbol{\chi}(r,\omega_N)$ is a complex number whose imaginary part accounts for the dissipation due to the field propagation [13]. Then, since in computing normal frequencies one drops dissipation effects, only the real parts of each element of $\boldsymbol{\chi}$, denoted by χ'_{ii}, are considered in what follows.

By substituting into Eq. (2) the assumed harmonic forms for $\boldsymbol{\mu}_{A,B}(t)$ and using Eq. (3), one obtains

$$\begin{aligned}\left(\omega_A^2 - \omega_N^2\right)\mu_{A,i} &= \zeta_A\chi'_{ii}(r,\omega_N)\mu_{B,i}\\ \left(\omega_B^2 - \omega_N^2\right)\mu_{B,i} &= \zeta_B\chi'_{ii}(r,\omega_N)\mu_{A,i}\end{aligned} \quad (5)$$

The existence of solutions of system (5) is ensured by the vanishing of its determinant, i.e., $(\omega_A^2 - \omega_N^2)(\omega_B^2 - \omega_N^2) - \zeta_A\zeta_B[\chi'_{ii}(r,\omega_N)]^2 = 0$. After trivial algebra, we get for each i two possible solutions for ω_N^2 that we call $\omega_{i,+}^2$ and $\omega_{i,-}^2$; these satisfy

$$\omega_{i,\pm}^2 - \tfrac{1}{2}\Big\{\left(\omega_A^2 + \omega_B^2\right) \pm \sqrt{\left(\omega_A^2 - \omega_B^2\right)^2 + 4\zeta_A\zeta_B[\chi'_{ii}(r,\omega_{i,\pm})]^2}\Big\} = 0. \quad (6)$$

By computing the normal frequencies $\omega_{i,\pm}$ of the system (2), we can rewrite it as a system of six uncoupled harmonic oscillators of frequencies $\omega_{i,\pm}$, $i = 1,2,3$ and energies $E_{i,\pm} = \omega_{i,\pm}J_{i,\pm}$, with $J_{i,\pm}$ the action constants depending on initial conditions. In Eq. (6), $\omega_{i,\pm}$ is given in a complicated implicit way. Explicit approximate expressions for $\omega_{i,\pm}$ are needed to compute the energy and then the interaction energy of the system of dipoles. In particular, we will see that *the range* of the interaction is strongly dependent on whether the dipoles oscillate at similar frequencies or not.

B. Off-resonance case

When $\omega_A \gg \omega_B$ (or when $\omega_A \ll \omega_B$), Eq. (6), for all i, becomes, at lowest order,

$$\omega_{i,\pm}^2 - \frac{1}{2}\left\{\left(\omega_A^2 + \omega_B^2\right) \pm \left(\omega_A^2 - \omega_B^2\right)\left(1 + \frac{2\zeta_A\zeta_B[\chi'_{ii}(r,\omega_{i,\pm})]^2}{\left(\omega_A^2 - \omega_B^2\right)^2}\right)\right\} \simeq 0,$$

which leads to

$$\underbrace{\omega_{i,\pm}^2 - \omega_{A,B}^2 \mp \frac{\zeta_A\zeta_B[\chi'_{ii}(r,\omega_{i,\pm})]^2}{\omega_A^2 - \omega_B^2}}_{\Theta_{i,\pm}(r,\omega_{i,\pm})} = 0 \text{ , where } \omega_{A,B} \text{ means } \begin{cases}\omega_A & \text{for } \omega_{i,+}\\ \omega_B & \text{for } \omega_{i,-}\end{cases}. \quad (7)$$

In Appendix B, we show how to solve the above equation by resorting to theorems of complex analysis including the Lagrange inversion theorem and Rouché's theorem. At the lowest order, the frequencies of the normal modes are given by the following formula:

$$\omega_{i,\pm}(r) \simeq \omega_{A,B} \pm \underbrace{\frac{\zeta_A\zeta_B(\chi'_{ii}(r,\omega_{A,B}))^2}{2\omega_{A,B}\left(\omega_A^2 - \omega_B^2\right)}}_{\Delta\omega_{A,B,i}(r)}. \quad (8)$$

The normal frequencies are equal to the frequencies of the dipole $\omega_{A,B}$ plus a shift due to the interaction. Note that $\omega_{A,B}$ corresponds to $\omega_{i,\pm}(r)$ when $\boldsymbol{\mu}_A$ and $\boldsymbol{\mu}_B$ are not interacting ($r \to \infty$). Let us also note that if the contour $\mathscr{C}$ had been chosen on the left part of the complex plane (complex numbers with negative real parts) when applying the argument principle, we would find the additive inverse of $\omega_{i,\pm}$ of Eq. (8). Finally, the dipole moments of the molecules, e.g., molecule A, can be given as

$$\mu_{A,i}(t) = \sum_i \mu^{(1)}_{A,i,+}e^{i\omega_{i,+}t} + \mu^{(2)}_{A,i,+}e^{-i\omega_{i,+}t} + \mu^{(1)}_{A,i,-}e^{i\omega_{i,-}t} + \mu^{(2)}_{A,i,-}e^{-i\omega_{i,-}t},$$

i.e., a sum of six uncoupled oscillators with frequencies $\omega_{i,\pm}$, $i = 1,2,3$ and mean energies $\omega_{i,\pm}J_{i,\pm}$ where $J_{i,\pm}$ are action constants depending on initial conditions. Therefore, the total average energy of the system is

$$\begin{aligned}E_{\mathrm{tot}} &= \sum_i E_{i,+} + E_{i,-} = \sum_i \omega_{i,+}J_{i,+} + \omega_{i,-}J_{i,-}\\ &= \underbrace{\sum_i \omega_A J_{i,+} + \omega_B J_{i,-}}_{\substack{\text{energy of the}\\ \text{uncoupled system}}} + \underbrace{\sum_i \Delta\omega_{A,i}(r)J_{i,+} - \Delta\omega_{B,i}(r)J_{i,-}}_{\text{interaction energy } U(r)},\end{aligned} \quad (9)$$

where the second sum is the interaction energy $U(r)$ of the system which, according to Eq. (8), scales linearly with $[\chi'_{ii}(r,\omega_{A,B})]^2$ in the off-resonance case. Thus, as a consequence of Eqs. (4), one gets

$$U(r) \propto \pm[\chi'_{ii}(r,\omega_{A,B})]^2 \sim \pm\frac{1}{r^6}, \tag{10}$$

in the limit $r \ll c/\omega_{A,B}$, i.e., the interaction potential $U(r)$ becomes short-range in the near zone limit. At very large intermolecular distance ($r \gg c/\omega_{A,B}$, i.e., far zone limits), it oscillates with a $1/r^2$ envelope. Let us remark that $U(r) \propto \frac{1}{r^6}$ is a van der Waals–like potential but not a true van der Waals potential which stems from virtual photon exchange, whereas our computation corresponds to a real exchange of electromagnetic energy.

C. Resonant case

When $\omega_A \simeq \omega_B = \omega_0$, Eq. (6) is simply reduced to

$$\underbrace{\omega_{i,\pm}^2 - \omega_0^2 \mp \sqrt{\zeta_A\zeta_B}\,\chi'_{ii}(r,\omega_{i,\pm})}_{\Theta_{i,\pm}(r,\omega_{i,\pm})} = 0. \tag{11}$$

Similarly to the nonresonant case, we can use arguments of complex analysis shown in Appendix B to estimate the frequencies of the normal modes at the lowest order:

$$\omega_{i,\pm}(r) \simeq \omega_0 \pm \underbrace{\sqrt{\zeta_A\zeta_B}\,\frac{\chi'_{ii}(r,\omega_0)}{2\omega_0}}_{\Delta\omega_{0,i}(r)}. \tag{12}$$

The first contribution to the frequency shift is now proportional to χ'_{ii}. In this case, the total energy is

$$E_{\text{tot}} = \underbrace{\sum_i \omega_0 J_{i,+} + \omega_0 J_{i,-}}_{\substack{\text{energy of the}\\ \text{uncoupled system}}} + \underbrace{\sum_i \Delta\omega_{0,i}(r)\left(J_{i,+} - J_{i,-}\right)}_{\text{interaction energy } U(r)}. \tag{13}$$

Thus, according to Eqs. (12) and (4), $U(r)$ will be a polynomial in $1/r^\alpha$ with $\alpha \leqslant 3$ (the dimension of physical space) making the potential long-range at all distance. Hence, intermolecular electrodynamic interactions between dipoles oscillating at similar frequencies are expected to have a much longer range of action with respect to off-resonance interactions. More specifically, from Eqs. (4) in the limit $r \ll c/\omega_0$ (near zone limit), and using Eqs. (13) and (12), the interaction energy as a function of the intermolecular distance is

$$U(r) \propto \pm\chi'_{ii}(r,\omega_{A,B}) \sim \pm\frac{1}{r^3} \tag{14}$$

because the term $1/r^3$ is dominant in the expression of $\chi'_{ii}(r,\omega)$ while in the intermediate and far zone limits the dominant contribution is a spatially oscillating one with a $1/r$ envelope [see the end of Appendix A for the functional form of $\chi'_{ii}(r,\omega)$].

III. NUMERICAL ESTIMATES OF RESONANT AND NONRESONANT INTERACTIONS BETWEEN BIOMOLECULES

A. Susceptibility and frequency shifts

To link up the above analytical results with the question of long-range molecular recognition in living matter, numerical estimation of resonance and off-resonance interactions is carried out using parameter values related to standard biomolecules. As discussed in more detail in the Sec. III C, there is a large body of literature about experimental evidences of low-frequency modes of vibration in the Raman and far-infrared spectra of polar proteins (see for example [14]). This is in line with our classical description since quantum effects become relevant when typical frequencies exceed $\omega \sim k_B T/\hbar = 3.92 \times 10^{13}$ Hz, at $T = 300$ K. For instance, one can set the resonance frequency ω_0 around 10^{11}–10^{12} Hz, as also suggested by Fröhlich [10,11]. To compute the coupling constants $\zeta = Q^2/m$, ten elementary charges and a mass of $m = 20$ kDa are taken as typical values for dipole moment and mass of small proteins (the same values are used for both molecules so that $\zeta_A = \zeta_B = \zeta$). As a first step in the estimation of the interaction potential $U(r)$, normal frequency shifts are computed in both resonant and nonresonant cases. From Eqs. (8) and (12), one has

$$\begin{aligned}\Delta\omega_{A,B,i}(r) &= \frac{\zeta^2[\chi'_{ii}(r,\omega_{A,B})]^2}{2\omega_{A,B}\left(\omega_A^2 - \omega_B^2\right)} \quad \text{when } \omega_A \gg \omega_B,\\ \Delta\omega_{0,i}(r) &= \zeta\frac{\chi'_{ii}(r,\omega_0)}{2\omega_0} \quad \text{when } \omega_A \simeq \omega_B = \omega_0,\end{aligned} \tag{15}$$

where the diagonal elements of the susceptibility matrix $\chi_{ii}(r,\omega)$ are given by Eq. (4) (the prime symbol stands for the real part). In Fig. 1, we have plotted the real parts of $\chi_{ii}(r,\omega)$ as a function of r for two values of ω, namely, $\omega = 10^{12}$ Hz and $\omega = 10^{16}$ Hz, below and above the classical-quantum limit, respectively. We are especially interested in $\chi_{ii}(r,\omega)$ when the intermolecular distance r is much larger than the dimensions of typical macromolecules, estimated around 5 nm, but less than cellular dimensions ~1–5 μm. The dielectric constant ε also appears in the expression of the susceptibility matrix as a function of the frequency. The real part of the dielectric constant of water is 80 in the electrostatic limit, i.e., $\omega \to 0$ but for large enough frequencies, typically larger than a dozen GHz [15], ε' drops to a few units, more exactly, $2 \leqslant \varepsilon' \leqslant 10$. As a compromise, we will assume $\varepsilon'(\omega) = 4$ for all ω we will consider in the following. As mentioned above, the elements of the susceptibility matrix were also plotted at very large frequency $\omega = 10^{16}$ Hz [Fig. 1(b)]. Even though quantum effects are important at such a frequency, quantum computations reveal that the "quantum" susceptibility matrix is the same as the classical one as well as its mathematical contribution to the interaction potential [6]. Very high frequencies might be relevant to account for certain dynamical properties of DNA molecules since a marked peak is observed in their polar spectra at wavelengths of 2600 Å, which is equivalent to a frequency $\omega \sim 7 \times 10^{15}$ Hz. When $\omega = 10^{12}$ Hz, it is seen from Fig. 1(a) that the $\chi'_{ii}(r,\omega)$'s are essentially monotonic

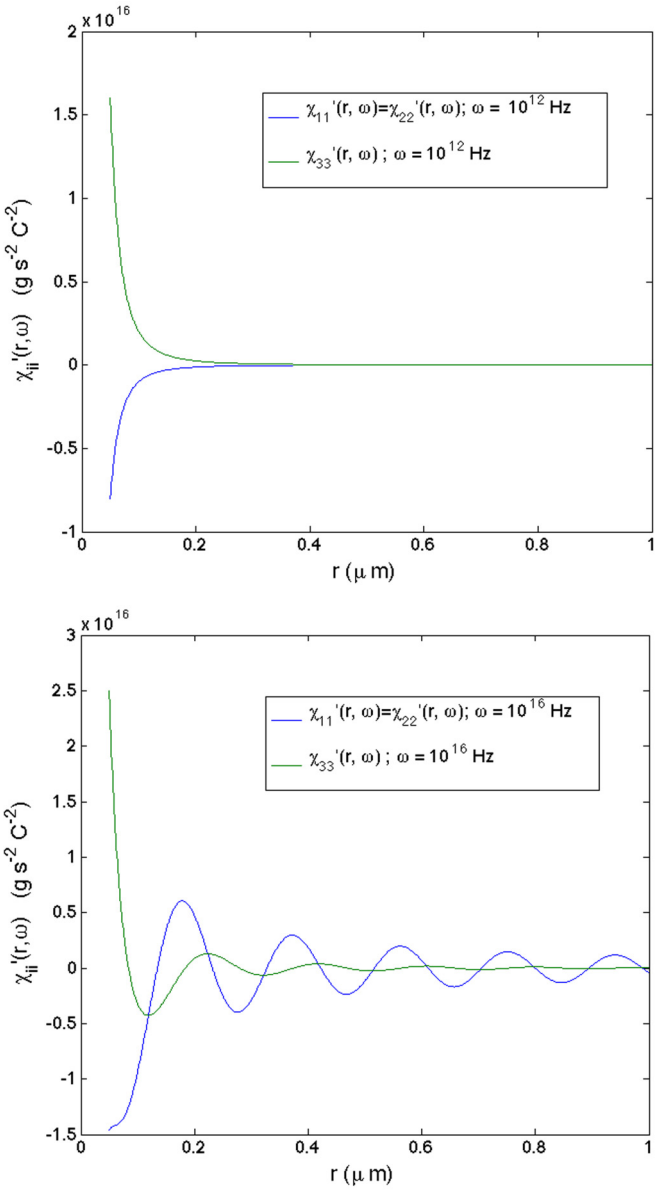

FIG. 1. (Color online) (a) Real part of the electric susceptibility matrix elements $\chi'_{ii}(r,\omega)$ computed from Eqs. (4) as a function of the distance r (the index E on χ_{ii} has been omitted to reduce the amount of notation). The parameter values are $\varepsilon'(\omega) = 1$ and $\omega = 10^{12}$ Hz. (b) Same as (a) except that $\omega = 7.24 \times 10^{15}$ Hz.

in r. The reason is that the intermolecular distance is much smaller than the characteristic wavelength $2\pi c/\omega$ of the electric field. From Eqs. (4), the susceptibility matrix elements are proportional to $1/r^3$ when $r \ll c/\omega$. In Fig. 1(b), the wavelength is small enough to observe oscillations at relatively short distances (less than 1 μm). At $r = 100$ nm, a frequency of at least $\omega_0 = c/r = 3 \times 10^{13}$ Hz is needed to observe field retardation effects.

The frequency shifts are estimated from Eq. (15) when the intermolecular distance is set to $r = 10$ nm and $r = 100$ nm. With the parameter values specified above, the frequency shifts of the transverse modes ($i = 1,2$) at resonance (with $\omega_0 = 10^{11}$ Hz) are found equal to 8.63×10^8 Hz and 8.63×10^5 Hz at $r = 10$ nm and $r = 100$ nm, respectively. To estimate off-resonance frequency shifts, a detuning $(\omega_A - \omega_B)/\omega_B = 10\%$, with $\omega_B = 10^{11}$ Hz, is used. Keeping the same values of the parameters, the frequency shifts of the transverse modes ($i = 1,2$) are found equal to 6.453×10^7 Hz and 64.53 Hz at $r = 10$ nm and $r = 100$ nm, respectively. Since the interaction potential is directly proportional to the frequency shifts in both resonant and nonresonant cases, it is found that dipolar interactions at resonance may exceed by several orders of magnitude off-resonance ones, typically when the distances become large with respect to biomolecular scale length (around 10–50 Å). This gap even widens by increasing the frequency of both dipoles.

B. Interaction energy and equivalent dipole overcoming thermal noise

For the sake of clarity, we will restrict ourselves to the resonant case. We recall the form of the resonant potential $U(r)$ derived in the previous sections [Eqs. (13) and (15)]:

$$U(r) = \sum_{i=1}^{3} \underbrace{\zeta \frac{\chi'_{ii}(r,\omega_0)}{2\omega_0}}_{\Delta\omega_{0,i}(r)} \underbrace{(J_{i,+} - J_{i,-})}_{\Delta J_i} \xrightarrow[r \ll c/\omega_0]{} \sum_{i=1}^{3} \zeta \frac{\sigma_i}{2\varepsilon'(\omega_0)\omega_0 r^3} \Delta J_i, \tag{16}$$

where $\sigma_1 = \sigma_2 = -1$ (transverse modes) and $\sigma_3 = 2$ (longitudinal mode), and the right hand side is obtained by using Eq. (4) when $r \ll c/\omega_0$. From Eq. (4), the potential goes as $1/r$ when $r \gg c/\omega_0$ but since r is supposed smaller than the cellular dimensions and the range $\omega_0 \sim 0.1$–1 THz is investigated, the limit $r \ll c/\omega_0$ will be considered. The interaction potential $U(r)$ requires the value of the actions $J_{i,\pm}$ of each normal mode. For a conservative system, actions are constant quantities which depend on initial conditions, i.e., on initial dipole moments and velocities of each molecule. However, biomacromolecules are nonlinear systems that may strongly interact with their environment resulting in long-lived nonequilibrium stationary states. Energy supply could also be well provided by cellular machinery [16,17] as discussed in Sec. III C (e.g., the energy released by the adenosine triphosphate (ATP) or the guanosine triphosphate (GTP) hydrolysis or the wasted energy released from mitochondria). Such conditions may lead to metastable states characterized by $J_{i,+}$ very different from $J_{i,-}$ whose values are not directly predictable from other physical quantities measured in equilibrium conditions (e.g., dipole moments of the molecules as they are estimated by *in vitro* experiments). Hence, estimating the exact values of $J_{i,+}$ and $J_{i,-}$ turns out to be a nontrivial task as it requires further investigation on how the molecules interact with their surrounding medium as well as a detailed description of the internal dynamics of the molecules, which is beyond the scope of this paper.

Even though the interaction energy cannot be estimated in an exact way, we can still compute it when the difference in the actions $\Delta J \sim \Delta J_i = J_{i,+} - J_{i,-}$ is of the order of thermal fluctuations, i.e., $\Delta J = k_B T/\omega_0$. This will provide a lower bound for the interaction potential. From Eq. (16), the

TABLE I. Numerical estimates of physical quantities connected with the interaction energy of two oscillating dipoles at resonance ($\omega_A \simeq \omega_B = \omega_0$). Grey columns correspond to parameters that were initially fixed. The temperature T and the dielectric constant ε' were set to 300 K and 4, respectively, for each estimate.

Z[a]	m (kDa)[b]	ω_0 (THz)[c]	r (nm)[d]	$\Delta\omega_0(r)$ (Hz)[e]	$\Delta x_{\max}$ (Å)[f]	μ (D)[g]	P (erg/s)[h]
10	10	0.1	10	1.7×10^{9}	17	813	1.6×10^{-12}
50	10	0.1	10	4.3×10^{10}	3	813	1.6×10^{-12}
50	100	0.1	10	4.3×10^{9}	3	813	1.6×10^{-12}
50	10	0.1	50	3.4×10^{8}	37	9099	2.0×10^{-10}
50	10	0.1	100	4.3×10^{7}	107	25737	1.6×10^{-9}
50	10	0.5	10	8.6×10^{9}	3	813	1.0×10^{-9}
50	10	0.5	100	8.6×10^{6}	107	25737	1.0×10^{-9}
10	10	1	10	1.7×10^{8}	16	813	1.0×10^{-6}
50	100	1	100	4.3×10^{5}	107	25737	1.6×10^{-5}
1000	50	0.1	100	3.4×10^{9}	0	25	1.6×10^{-9}

[a] Z: number of charges with $Q = Ze$.
[b] m: mass in kilodaltons (kDa).
[c] ω_0: resonance frequency.
[d] r: intermolecular distance.
[e] $\Delta\omega_0(r)$: frequency shift due to dipolar interactions. Computed from Eq. (15).
[f] $\Delta x_{\max}$: maximum amplitude that should carry any of the dipoles so that dipole interactions overcome thermal noise at separation r. Computed from Eq. (19).
[g] $\mu = Q\Delta x_{\max}$: maximum dipole moment required to overcome thermal noise at r.
[h] P: Power radiated by one dipole in case interactions overcome thermal noise at separation r. Computed from Eq. (20).

interaction energy becomes $U(r) \sim \Delta\omega_{0,i}(r)k_BT/\omega_0$. Using the estimates of the frequency shifts $\Delta\omega_{0,i}(r)$ found in the last subsection for the transverse normal modes, we find that $U(r)$ is equal to 3.57×10^{-16} erg and 3.57×10^{-19} erg, at $r = 10$ nm and $r = 100$ nm, respectively. These values should be compared with the value of $kT = 4.14 \times 10^{-14}$ erg at 300 K, which reveals that ΔJ should be at least two orders of magnitude larger than the Boltzmann action so that dipole interactions balance exactly thermal energy at $r = 10$ nm. To give an idea of what two orders of magnitude means in terms of action variables, we can compute the dipole moment equivalent to a given value of ΔJ. Writing

$$\omega_0\Delta J = \frac{(\Delta p)^2}{2m} + \frac{1}{2}m\omega_0^2(\Delta x)^2, \tag{17}$$

where we assumed $m_A = m_B = m$ for simplicity, the dipole displacement Δx is maximum when $\Delta p = 0$, so that

$$\Delta x_{\max} = \sqrt{\frac{2\Delta J}{m\omega_0}}. \tag{18}$$

Again, dipole interactions overcome thermal noise when $U(r) \sim k_BT$, that is, $\Delta J = k_BT/\Delta\omega_0(r)$ where $\Delta\omega_0(r)$ is given by Eq. (16) (the subscripts i are omitted as, roughly speaking, each component has the same order of magnitude). Using Eq. (15), the maximum amplitude of the equivalent dipole is given by

$$\Delta x_{\max} = 2\sqrt{\frac{k_BT}{Q^2\chi'(r,\omega_0)}} \xrightarrow[r\ll c/\omega_0]{} 2\sqrt{\frac{k_BTr^3\varepsilon'(\omega_0)}{Q^2}}, \tag{19}$$

where we have used $\zeta = Q^2/m$ and, using Eq. (4), replace $\chi'(r,\omega_0)$ by its limit when $r \ll c/\omega_0$. $\Delta x_{\max}$ can be interpreted as the maximum amplitude that should exhibit any of the dipoles so that resonant interactions balance exactly thermal fluctuations at a given r. Using parameter values introduced above (Q given by ten elementary charges, $\varepsilon'(\omega_0) = 4$), we find that $\Delta x_{\max} = 1.694 \times 10^{-7}$ cm $= 16.9$ Å at $r = 10$ nm. The corresponding dipole moment is $\mu = Q\Delta x_{\max} = 8.1388 \times 10^{-16}$ statC cm $= 813.88$ D. The larger the value of Q, the smaller the value of the polar amplitude $\Delta x_{\max}$. For instance, when Q is given by 50 elementary charges, $\Delta x_{\max} = 3.389\,05 \times 10^{-8}$ cm $= 3.389\,05$ Å at $r = 10$ nm while the equivalent dipole moment μ remains the same. Table I gives a summary of the numerical estimates discussed so far plus other estimates obtained by varying parameters such as the intermolecular distance or the resonance frequency. In a recent paper [18], molecular dynamics simulations performed for an ensemble of interacting molecules reveal that $1/r^3$ resonant interactions might already have a profound influence on the diffusion dynamics when the interacting energy is equal to $kT/10$ at $r = 100$ nm. Substituting kT with $kT/10$ in Eq. (19), we find that the equivalent dipole moment $\mu = Q\Delta x_{\max}$ is equal to 8138.8 D when $r = 100$ nm. This value together with the values of the dipoles moments given in the table can appear to be very large in comparison with the dipole moments of a wide class of proteins given around a few hundred debyes [19,20]. However, a mathematical approach similar to the one of Sec. II might be applied to estimate the interaction energy between two sets of oscillating dipoles instead of two single ones. Since we should take care of the local density of dipoles, the dynamical variables will be no longer the dipole moments of the molecules but the polarization fields, e.g., $P_A = n_A\langle\mu_A\rangle$, with n_A the number of dipoles making up the "molecule" A with an average dipole moment $\langle\mu_A\rangle$ (and similarly for the "molecule" B). Assuming that the dipoles of each molecule oscillate in phase, one can estimate the maximum amplitude that should carry any

of the dipoles so that resonant interactions balance thermal noise at distance r. Similarly to the above computations, we can show that $\Delta x_{\max} = 2\sqrt{k_B T r^3 \varepsilon'(\omega_0)/n^2 Q^2}$, where we have supposed that the number of dipoles composing each molecule was approximatively the same ($n_A \simeq n_B = n$). In this case, the average dipole amplitude is n times less than the amplitude required by single dipoles, which might lead to more realistic values of the dipole moments when n is large. At the same time, the frequency shifts in the case of two interacting sets of dipoles should be computed according to Eq. (15) with coupling constants given by $\zeta = nQ^2/m$ instead of Q^2/m. A possible value for n could be well given by the number of water molecules surrounding protein structures [21]. It has been recently demonstrated by the work of Pollack [22] that hydrophilic surfaces have long-range effects on aqueous solutions containing solute molecules. The so-called "exclusion zone" (EZ) is created by repulsive forces extending over distances of many Debye lengths, possibly on the μm scale. Since proteins are typically structured with a hydrophobic core and a hydrophilic exterior surface, it is expected that similar EZ effects occur in the case of proteins and protein aggregations. One of the characteristics of the water molecules surrounding biomolecules such as proteins and DNA is the formation of several ordered layers of water surrounding a biomolecule [23]. These layers exhibit electrostatic ordering and also structural organization, possibly involving a hexatic lattice [24]. These phenomena may all be linked and can be interpreted in the spirit of the Mercedes-Benz model of water [25] whereby a charged (hydrophilic) surface such as that of a protein attracts the oppositely charged orbital of a water molecule leaving the remaining three orbitals free to explore rotational freedom in the plane approximately parallel to the charged surface of the protein. The so-formed hexatic arrangements of water orbitals resemble helicopter blades or the logo of Mercedes-Benz, hence the name of the model. This suggests a very interesting phenomenon since these positionally localized water molecules possess a dipole moment that is free to rotate around the axis roughly perpendicular to the protein surface. These rotating dipole moments should undergo precessional motion if there is a sufficiently strong electric field created, for example, by the charge distribution of the protein. For instance, in the case of tubulin, its net dipole moment is of the order of 1000–5000 D [26] depending on the tubulin isoform. This then leads to a dynamic picture of thousands of water molecules with their dipole moments precessing at a frequency in the 10^{11}-Hz domain which is sensitive to the electric field generated by the biomolecular surface. The latter should also depend on the environmental conditions (pH, ion concentrations, salt concentration, and so on). Moreover, conformational changes in the states of a protein still affect the magnitude and direction of the electric field that drives the dynamics of these precessing dipoles. Therefore, this could serve as a mechanism for selective generation of attractive or repulsive forces between interacting proteins (with their water of hydration). The electric field of the protein may additionally exhibit vibrational modes due to collective excitation modes, $\mathbf{E} = \mathbf{E}_0 + \mathbf{E}_1 e^{i\omega t}$. This, through coupling with dipole moments of the water molecules, will result in the slaving of water dynamics to the collective dynamics of the protein and generate coherent vibrational dynamics of dipole moments. This scenario offers a possible role of water dynamics in living processes.

C. The question of damping

Different physical processes may lead to a partial or complete dissipation of an electrodynamic signal in a solvent and therefore should be discussed openly to assess the role of long-range electrodynamic forces between biomolecular structures. As discussed in the Introduction, an electrolyte such as the cell cytoplasm behaves as a pure dielectric when electromagnetic fields with frequencies larger than 250 MHz are involved. In this context, the origin of the damping of electrodynamic forces is threefold:

(1) Radiation losses.
(2) Dielectric absorption.
(3) Solvent viscosity.

Radiation losses. The total instantaneous power P radiated by an oscillating charge Q is given by the Larmor formula [27,28]

$$P = \frac{2}{3}\frac{Q^2|\ddot{\mathbf{x}}|^2}{c^3}, \tag{20}$$

where $Q = Ze$ and the acceleration is given by $\ddot{\mathbf{x}} = -\omega_0^2 \mathbf{x}$. The maximum amplitude $\Delta x_{\max}$ of a dipole such that the interaction energy is approximately $k_B T$ at separation r is given by formula (19). Substituting x for $\Delta x_{\max}$ in the last equation, we get

$$P = \frac{8}{3}\frac{k_B T r^3 \omega^4 \varepsilon'(\omega)}{c^3}. \tag{21}$$

The last column of Table I gives numerical estimates of P typically when $\omega \sim 0.1$–1 THz and $r \sim 10$–100 nm. Those values of P should be compared for example with the power potentially available from ATP hydrolysis in the cell. The typical intracellular concentration of ATP molecules is given around 1 mM implying that a protein molecule in the cell undergoes around 10^6 collisions with ATP molecules per second [29]. Given the standard free energy obtained from ATP hydrolysis estimated around 50 kJ mol^{-1} $= 8.306 \times 10^{-13}$ erg, we can assume that 1% of the collisions with ATP will provide energy, which corresponds to a power supply of 8.306×10^{-9} erg s^{-1} potentially available. From Table I, we see that some parameter values are not suitable to sustain electrodynamic interactions over long distances. Clearly, when $\omega = 1$ THz, the power radiated becomes very large even at smaller separations $r = 10$ nm. When $r = 10$ nm, $P = 1.636 \times 10^{-8}$erg s^{-1} whereas when $r = 100$ nm, $P = 1.636 \times 10^{-5}$erg s^{-1} which is much larger than the power supplied by ATP hydrolysis. On the other hand, when $\omega = 0.1$ THz, P is estimated less than or around 10^{-9} erg s^{-1} up to $r = 100$ nm, which is still in support of long-range electrodynamic interactions. At intermediate frequencies $\omega = 0.5$ THz, electrodynamic interactions can be still considered when intermolecular distances are given around $r = 10$ nm but not when $r = 100$ nm. Typical frequencies above which electrodynamic interactions between single dipoles are hardly maintainable because of radiation losses (i.e., $P > 10^{-8}$ erg s^{-1}) are 1.501

and 0.266 THz when $r = 10$ nm and $r = 100$ nm, respectively. Besides ATP hydrolysis, other possible forms of energy supply should be considered in a cellular environment. In Ref. [16], a detailed analysis of possible sources of energy to excite and sustain coherent vibrations in microtubules is given, for example, the energy transferred from moving of motor proteins along microtubules with a power supply estimated around 4×10^{-8} erg s^{-1}, or the energy released from mitochondria as "wasted" energy in the course of a citric acid cycle with a power supply given around 10^{-7} erg s^{-1}. Both sources of energy might well be enough to excite long-range biomolecular forces as the corresponding powers are around or larger than the power considered above for ATP hydrolysis.

One may consider the possibility that long dipolar interactions would drive specific biomolecular encounters in response to a particular external excitation thus requiring that resonant forces are only active during a short period of time. Hence, occasional energy supply rather than constant energy inputs would be enough to sustain the large dipole moments needed. An estimate of the typical encounter time of two biomolecular structures driven by an intermolecular potential $U(r)$ can be directly deduced from the association rate k_a of molecules in a solution of initial concentration $\mathcal{C}$, where $\mathcal{C} = 1/r^3$ and r is the range of intermolecular distances of interest. k_a is given by the Smoluchovski-Debye formula [30,31]:

$$k_a = 4\pi R^*(D_A + D_B),$$
$$R^* = \frac{1}{\displaystyle\int_{(R_A+R_B)/2}^{\infty} \frac{e^{U(x)/kT}}{x^2} dx}, \quad \text{and} \quad D_{A,B} = \frac{kT}{\gamma_{A,B}}. \tag{22}$$

As usual, the friction coefficient $\gamma_{A,B}$ of each molecule can be approximated from Stokes law: $\gamma_{A,B} = 6\pi\eta R_{A,B}$ where $\eta \simeq 10^{-2}$ g cm^{-1} s^{-1} is the dynamic viscosity of water at 300 K. We also set $R_A = R_B = 1$ nm as a typical radius for small proteins and $U(x)$ is given from Eq. (16) so that $U(x = r) \simeq kT$. Similarly to the computations done so far, we set $U(x) = \Delta\omega_{0,i}(x)kT/\Delta\omega_{0,i}(r) = -kT(r/x)^3$. The characteristic half-life of the A-B reaction can be written as $\tau = 1/k_a\mathcal{C}$. Using Eq. (22), $\mathcal{C} = 1/r^3$ and the values of the parameters introduced above, we find that $\tau = 1.617 \times 10^{-8}$–$1.617 \times 10^{-6}$ s when $r = 10$–100 nm, respectively [note that in the Brownian case, $U(x) = 0$, $\tau = 9.05 \times 10^{-8}$–$9.05 \times 10^{-5}$ s, respectively]. Assuming that we provide to each molecule involved an energy equivalent to a single ATP hydrolysis, i.e., $\Delta E_{\mathrm{ATP}} = 8.306 \times 10^{-13}$ erg [32], we find a power equivalent to $P_{\mathrm{ATP}} = \Delta E_{\mathrm{ATP}}/\tau = 5.136 \times 10^{-7}$ erg/s when $r = 100$ nm. Comparing with the power radiated by one dipole (last column of Table I), we see that dipoles oscillating with a frequency less than $\sim$1 THz use a power much smaller than P_{ATP}, thus showing that an energy equivalent to a single ATP hydrolysis for each protein is more than enough to compensate radiation losses during the typical encounter time of biological partners.

Among possible sources of energy, ultraweak photons constitute ideal candidates. At the cellular and subcellular level, living systems are known to emit ultraweak endogenous photons without the need for external excitation [33–41]. This is only dependent on the presence of metabolic activity. These electromagnetic excitations are produced via various biochemical reactions, but principally from bioluminescent radical recombination reactions involving the very numerous reactive oxygen and nitrogen species which results in a subsequent relaxation of excited states giving rise to photon emission. The oxidative phosphorylation metabolism taking place in the mitochondria of living cells and lipid peroxidation appear to be a primary source for this activity [42,43]. Oxidative phosphorylation is the most common form of energy production in dividing cells. Neurons also continuously produce photons during their ordinary metabolism [44,45], and it has been shown *in vivo* that the intensity of photon emission from rat brain correlates well with cerebral energy metabolism, electrical activity, blood flow, and oxidative stress [37,46]. Moreover, Sun *et al.* [47] demonstrated that ultraweak bioluminescent photons can propagate along neural fibers and can be considered a means of neural communication. Also of interest is the reported radical recombination within mitochondria which can emit photons in the UV range required to excite the chromophoric network within microtubules [48].

Dielectric absorption. So far, only the real part of the dielectric constant has been considered as it is part of the expression of the interaction potential $U(r)$. The imaginary part of ε should be also taken into account to describe the ability of a dielectric medium to absorb electromagnetic waves. The absorbance $\alpha(\omega)$ is generally used to describe dielectric losses and is given as $4\pi n''(\omega)/\lambda$ where n'' is the imaginary part of the refractive index $n(\omega) = n'(\omega) + in''(\omega)$. At the same time, the refractive index is related to the dielectric constant through the following relations:

$$\varepsilon'(\omega) = n'(\omega)^2 - n''(\omega)^2\varepsilon''(\omega) = 2n'(\omega)n''(\omega), \tag{23}$$

thus yielding the following expression for the absorbance:

$$\alpha(\omega) = \frac{2\omega}{c}\left(\frac{\sqrt{\varepsilon'(\omega)^2 - \varepsilon''(\omega)^2} - \varepsilon'(\omega)}{2}\right)^{1/2}. \tag{24}$$

Most experiments done on polar liquids show that the dielectric spectrum of water is characterized by two relaxation times τ_1 and τ_2 and can be easily fitted with a Debye-like relaxation formula in the far infrared region [49,50]:

$$\varepsilon(\omega) = \varepsilon_\infty + \frac{\varepsilon_s - \varepsilon_1}{1 + (i\omega\tau_1)} + \frac{\varepsilon_1 - \varepsilon_\infty}{1 + (i\omega\tau_2)}. \tag{25}$$

Here, ε_s and ε_∞ are the static and high-frequency dielectric constants and ε_1 is an intermediate step in the dielectric constant. For water, the critical frequencies $\omega_1 = \tau_1^{-1}$ and $\omega_2 = \tau_2^{-1}$ are estimated around $\omega_1 = 0.12$ THz and $\omega_2 = 5.56$ THz, respectively. Investigating the absorbance of water from Eq. (24) or experimentally, it is found that $\alpha(\omega)$ increases drastically when $\omega < \omega_1$ or so and increases more slowly when $\omega > \omega_1$ (see Fig. 2). Numerical estimates of the absorbance when $\omega = 0.1$ THz and $\omega = 1$ THz are $\alpha = 16.25$ cm^{-1} and $\alpha = 103.125$ cm^{-1}, respectively, leading to typical penetration lengths $\delta = 1/\alpha$ equal to 615.3 and 96.9 μm, respectively. A similar range around 50–150 μm for the penetration length δ is found for most biological tissues when $\omega = 0.1$–1 THz [51]. Coming back to the problem of long-range intermolecular interactions, typical distances between biopartners are supposed to be much less than cellular dimension ($<$1–5 μm). Hence, damping due to dielectric losses can be neglected in the present case.

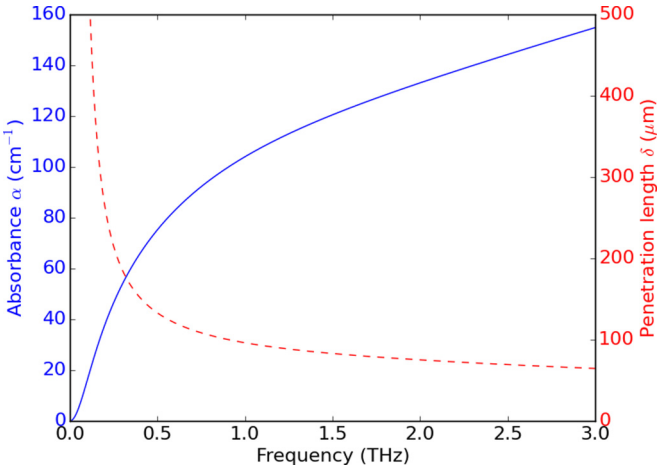

FIG. 2. (Color online) Absorbance of water in the terahertz domain (blue). Penetration length as a function of the frequency (red).

Let us remark that a theoretical result [52] predicts that the electromagnetic near field of a Hertzian dipole immersed in a dissipative medium is strongly damped. In other words, a Hertzian dipole could not sustain, according to the authors of the mentioned work, its oscillation in a dissipative medium to maintain a finite field at a distance. This effect stems from Eq. (10) of Ref. [52]. However, in the absence of both experimental evidence and a physical explanation of the singularities shown by this equation, it is still unclear whether this analysis applies at the molecular level.

Solvent viscosity. Compared with other possible dissipation mechanisms, the question of the damping of biomolecular vibrations due to the viscosity with the surrounding medium is probably one of the most controversial when discussing possible long-range effects in biological systems. The first measurements of low-frequency vibrations of proteins in the Terahertz domain date back to the 1970s and were carried out via Raman spectroscopy. Although spectral studies of proteins in their crystal state show significant low-frequency bands around 1 THz (for example, around 0.75 THz for a protein of lysozyme or around 0.42 THz for a molecule of bovine serum albumin (BSA)), the low-frequency Raman bands are hardly observed when the proteins are immersed in water [53,54]. Based on hydrodynamic arguments, many authors suggest that the disappearance of the low-frequency Raman band in solution indicates overdamping of the corresponding oscillations [55]. However, estimates of the damping coefficient usually employ the Stokes formula, which can hardly be used when the amplitude of oscillations is comparable with the linear dimensions of water molecules forming a continuous medium [56]. Other theoretical studies based on estimates of a typical absorption cross section of water-protein interactions [32,57,58] also reach the conclusion that protein vibrations would be strongly damped by contact with their aqueous biological environment. All the above mentioned analyses have in common that the solvent is always considered to play a passive role in the dynamics of the proteins. However, new experimental techniques based on terahertz spectroscopy can quantify how water interacts with biomolecules and, in doing so, show that the dynamics of hydration water in the vicinity of protein surfaces—the so-called hydration shell—differs from "bulk" water in that it correlates with protein motion [59]. Applying hydrodynamic arguments in the framework of microtubule dynamics, Pokorný showed that if instead of the commonly used no slip condition at the surface of molecules, slip boundaries for microtubules' longitudinal vibrations are taken into account, vibrations may be still excited [60]. In the course of considering resonances in the DNA microwave absorption spectra reported in Ref. [61] and first interpreted as sound waves, Van Zandt [62,63] revisited the subject and concluded that a layered structure of water imposed by the interaction between DNA with polar molecules of the solvent gives a reduction in the DNA longitudinal sound damping like that observed in [61]. According to Van Zandt's estimates, such vibrations might have a dissipation time of the order of $\tau = 5$ ns. Since the appearance of new terahertz detection techniques, evidences of underdamped low-frequency vibration modes of proteins become more and more frequent. For example, Gruia *et al.* [64] have reported using femtosecond coherence spectroscopy that ferric heme proteins exhibit dominant oscillations near 40 $cm^{-1} = 1.2$ THz characterized by a factor Q of four to five units (the factor Q represents approximatively the number of oscillations performed by an oscillator before being completely damped; typically when $Q > 0.5$, an oscillation mode can be considered underdamped, otherwise it is overdamped). Cimei *et al.* [65] have used pump-probe experiments to detect underdamped modes of vibration of azurin, a blue copper protein, in the 30–80-cm^{-1} region. Using extremely sensitive femtosecond optical Kerr-effect spectroscopy, Turton *et al.* have found that underdamped modes (with a Q factor of a few units) might be involved in the efficiency of lysozyme-ligand interactions [66]. An exceptionally long-lived mode of vibration exhibiting around 1500 oscillations (over 500 ps) before complete damping was observed for the bacteriorhodopsin at frequencies around 2 THz [67]. It should also be mentioned that molecular dynamics (MD) simulations predict Q factors larger than ten units for small molecules vibrating in the range of terahertz [56,68]. The smaller the size and mass of the molecules of solvent (or of their clusters) in comparison with those of the subglobule, the smaller is the Q factor of the subglobular oscillations.

Summarizing, solvent viscosity turns out to be the most likely source of damping of electromagnetic signals in a biological context compared with radiation losses and dielectric absorption. However, numerous theoretical and experimental evidences of underdamped modes of vibration of biomolecular structures are reported in the literature, in which case water is expected to contribute actively to the dynamics of the molecules. Among all experimental studies done so far, the bacteriorhodopsin has been found to exhibit the most persistent vibrational motion in the terahertz domain over a time of 500 ps whereas an important variety of other proteins is characterized by Q factors of a few units associated with low-frequency vibration modes. Since resonant forces as those derived in the previous sections occur quasi-instantly when large enough dipole oscillations are excited, underdamped protein modes even with small Q might still contribute, even temporarily, to long-distance intermolecular interactions. In the framework of biomolecular recruitment to ensure particular cellular functions, it can be speculated that interactions are activated at intervals to guide specific proteins to their biological targets.

Whenever long-distance interactions become inactive due to the friction with the surrounding medium, local chemical forces and Brownian motion would entirely contribute to the diffusion dynamics of the molecules. How often long-range forces are activated might depend on how often energy is provided to those systems. In an environment as viscous, heterogeneous and anisotropic as the cellular environment, it is not obvious that Brownian motion is sufficient to bring specific cognate partners at the same place in a time short enough to meet physiological needs. Long-range forces, even occasionally active, may be relevant to facilitate and preserve order in the cell. Detailed investigation on how long-range electrodynamic forces could improve cellular organization is beyond the scope of the present paper.

IV. COMPARISON BETWEEN CLASSICAL AND QUANTUM ELECTRODYNAMIC INTERACTIONS

Now that the interaction energy of system (2) has been worked out, it is of interest to note that the interaction energies $U_\pm$ computed from Eqs. (9) or (13) as

$$U_\pm(r) = \hbar \sum_i [\omega_{i,\pm}(r) - \omega_{A,B}], \tag{26}$$

i.e., with the substitutions $J_{i,+} = \hbar$, $J_{i,-} = 0$, or $J_{i,+} = 0$, $J_{i,-} = \hbar$, respectively, correspond exactly to the interaction energy (due to *real* photons) between two neutral atoms when one of them is in an excited state. This is fully consistent with the idea that atoms and the radiation field mediating the interaction are generally described as an ensemble of coupled oscillators whereas normal modes and susceptibilities are the same for classical and quantum oscillators. However, despite this remarkable analogy, of course, the origin of the interactions is totally different. Whereas atomic dipoles in the QED framework are associated with electronic transitions, the classical computations mainly apply to dipole oscillations associated with conformational vibrations of macromolecules. In what follows, the classical-quantum correspondence of electrodynamic interactions is given more explicitly in both nonresonant and resonant cases.

A. Off-resonance case

Off resonance, the normal frequencies are given by Eq. (8) so that $U_\pm$ reads as

$$U_+(r) = \frac{\hbar}{2\omega_A} \frac{\zeta_A \zeta_B}{\omega_A^2 - \omega_B^2} \sum_i (\chi'_{ii}(r,\omega_A))^2 \tag{27}$$

and

$$U_-(r) = \frac{\hbar}{2\omega_B} \frac{\zeta_A \zeta_B}{\omega_B^2 - \omega_A^2} \sum_i (\chi'_{ii}(r,\omega_B))^2. \tag{28}$$

Again, the components of the electric susceptibility $\chi_{ii}(r,\omega)$ are given by Eq. (4) but have not been made explicit here for the sake of clarity. Even if Eqs. (27) and (28) were obtained classically, $U_\pm(r)$ would be equivalent to the energy shifts due to the interaction between two atoms A and B with distinct transition frequencies $\omega_A \neq \omega_B$ when one of the atoms is in an excited state [$U_+(r)$ is the energy shift when the atom A is excited whereas $U_-(r)$ is when the atom B is excited]. The analogy is better seen writing $\alpha^{A,B}_{\text{class.}}(\omega)$, the classical polarizabilities of each dipole, such that

$$\alpha^{A,B}_{\text{class.}}(\omega) := \frac{\zeta_{A,B}}{\omega_{A,B}^2 - \omega^2}. \tag{29}$$

In this case, $U_\pm(r)$ has exactly the same form as the quantum shifts computed, for example, by Gomberoff *et al.* [see Eq. (44) in Ref. [69]; see also [70]] in the context mentioned above. U_+ is the energy shift associated with the (approximated) wave function $|\psi_+\rangle = |e_A, g_B\rangle$ whereas U_- is the energy shift associated with $|\psi_-\rangle = |g_A, e_B\rangle$ (here we have noted e_A or g_A when the atom A is excited or is in its ground state, respectively, the atoms A and B being uncoupled, and similarly for B). Finally, we should remark that the classical computations carried out above do not allow us to reproduce the QED contribution in the energy shift due to virtual photons, i.e., which accounts for the interaction between the ground states of two atoms. As shown explicitly in Ref. [71], such a contribution purely arises from vacuum fluctuations. A fully quantum description is then needed to derive the corresponding potential (see also Refs. [72] for other derivations of van der Waals forces between two ground state atoms).

B. Resonant case

At resonance, i.e., when $\omega_A \simeq \omega_B = \omega_0$, the normal frequencies are given by Eq. (12) so that $U_\pm$ is simply

$$U_\pm(r) = \pm \frac{\hbar}{2\omega_0} \sqrt{\zeta_A \zeta_B} \sum_i \chi'_{ii}(r,\omega_0). \tag{30}$$

Here, $U_\pm(r)$, with $\chi_{ii}(r,\omega)$ given from Eq. (4), is the classical equivalent of the interaction energy between two two-level atoms in an excited state with a common transition frequency ω_0. The quantum result is usually given in terms of the off-diagonal elements of the dipole operator in the unperturbed state $\mu_A^{ge} = \langle g_A|\hat{\mu}_A|e_A\rangle$ and $\mu_B^{ge} = \langle g_B|\hat{\mu}_B|e_B\rangle$ (here we have supposed a condition of isotropy for the dipole moment of both atoms). In addition, let us remind that the *quantum* polarizability $\alpha_{\text{quant.}}$ depends on these elements such that

$$\alpha^{A,B}_{\text{quant.}}(\omega) := \frac{2}{3\hbar} \frac{\omega_{A,B} \left(\mu^{ge}_{A,B}\right)^2}{\omega_{A,B}^2 - \omega^2}. \tag{31}$$

Thus comparing Eqs. (31) and Eqs. (29) in the resonant case, one gets the following classical/quantum equivalence:

$$\zeta_{A,B} \rightsquigarrow \frac{2}{3\hbar} \omega_0 \left(\mu^{ge}_{A,B}\right)^2,$$

with $\omega_A \simeq \omega_B = \omega_0$, so that the quantum version of $U_\pm$ can be easily derived:

$$U_\pm(r) = \underbrace{\pm \frac{\hbar}{2\omega_0} \sqrt{\zeta_A \zeta_B} \sum_i \chi'_{ii}(r,\omega_0)}_{\text{classical}} \rightsquigarrow \underbrace{\pm \frac{1}{3} \mu_A^{ge} \mu_B^{ge} \sum_i \chi'_{ii}(r,\omega_0)}_{\text{quantum}}.$$

The last term corresponds exactly to the quantum energy shifts given for example by Eq. (5) in Ref. [4] [see also Eq. (2.27) in Ref. [4]] whose approximated eigenstates are

$$|\psi_+\rangle = \frac{1}{\sqrt{2}}[|e_A,g_B\rangle - |g_A,e_B\rangle] \quad \text{and}$$
$$|\psi_-\rangle = \frac{1}{\sqrt{2}}[|e_A,g_B\rangle + |g_A,e_B\rangle], \tag{32}$$

for U_+ and $U-$, respectively. Again, let us emphasize that the interaction potential at resonance is of a much longer range than the off-resonance one. From a biological point of view, such frequency-selective interactions could be of utmost importance during the approach of a molecule toward its specific target as mentioned in the Introduction. On the other hand, quantum states given by Eqs. (32), as entangled (excitonic) states are fragile. In living matter, a noisy cellular environment could be sufficient to entail decoherence over long distances making long-range interactions between atoms not very probable in this case. In this way, classical computations have the advantage of getting rid of the problem of quantum coherence, since, in this case, dipole moments of biomolecules are associated to classical conformational vibrations rather than electronic transitions. Again, this is in line with the experimental observations of low-frequency oscillations modes in the Raman and far-infrared spectra of polar proteins. These spectral features are commonly attributed to collective oscillation modes of the whole molecule (protein or DNA) or of a substantial fraction of its atoms.

V. LONG-RANGE ELECTRODYNAMIC INTERACTIONS AT THERMAL EQUILIBRIUM

Long-range interactions between two biological dipoles were originally considered by Fröhlich [8,11]. Fröhlich emphasized, *inter alia*, that long-range interactions may occur at resonance even though the system of dipoles is close to thermal equilibrium. In a biological context this could be problematic as switching on and off long-range recruitment forces seems more fit to explain activation and inhibition processes at work at the molecular level in living matter. To clarify this point, let us consider the dipoles $\boldsymbol{\mu}_A$ and $\boldsymbol{\mu}_B$ of system (2) in thermal equilibrium and suppose that $\hbar\omega_{A,B} \ll k_BT$ so that classical effects are dominant (as discussed in Sec. III, this implies frequencies less than $k_BT/\hbar = 3.92 \times 10^{13}$ Hz at $T = 300$ K, which is in agreement with experimental evidence of marked peaks in the vibration spectra of many proteins [14]). For a system interacting with a thermal bath, the interaction energy is best described by the difference of free energies between the interacting system and the noninteracting one: $U(r) = F(r) - F(\infty) = -k_BT \ln[Z(r)/Z(\infty)]$, where $Z(r)$ is the partition function of the system when the dipoles are separated by a distance r. In thermal equilibrium, the partition function is computed from Boltzmann weights. This can be easily calculated in the space of the normal modes as those are equivalent to uncoupled harmonic oscillators:

$$Z(r) = \prod_{i=1}^{3} \int \cdots \int d\pi_{i,+}d\pi_{i,-}d\mu_{i,+}d\mu_{i,-} \exp\left[-\frac{\pi_{i,+}^2 + \omega_{i,+}^2(r)\mu_{i,+}^2}{2k_BT}\right]$$
$$\times \exp\left[-\frac{\pi_{i,-}^2 + \omega_{i,-}^2(r)\mu_{i,-}^2}{2k_BT}\right] = \prod_{i=1}^{3} \frac{(2\pi k_BT)^2}{\omega_{i,+}(r)\omega_{i,-}(r)}, \tag{33}$$

where $\pi_{i,\pm}$ and $\mu_{i,\pm}$ stand for the components of normal coordinates related to momenta and positions, respectively. Possible nonlinear contributions of the potential due to dipole anharmonicities, as mentioned at the beginning of Sec. II, have been omitted as they are supposed to be negligible compared with the harmonic part of the potential.

Thus the free energy difference is given by (see also Ref. [11])

$$U(r) = k_BT \sum_i \ln\left[\frac{\omega_{i,+}(r)\omega_{i,-}(r)}{\omega_A\omega_B}\right], \tag{34}$$

with $\lim_{r\to+\infty} \omega_{i,\pm}(r) = \omega_{A,B}, \forall i$. To derive Fröhlich results, we consider the resonant case $\omega_A \simeq \omega_B = \omega_0$, and substitute $\omega_{i,\pm}(r)$ in Eq. (34) with their *implicit* form [Eq. (11)]. At long distances, we can use Taylor expansion: $\ln(1+x) \sim x$. One gets the formula of the interaction energy given by Fröhlich by making explicit the susceptibility matrix elements χ_{ii} from Eq. (4) when $r \ll c/\omega_0$. One obtains

$$U(r) \simeq \frac{k_BT\sqrt{\zeta_A\zeta_B}}{2\omega_0^2}\frac{1}{r^3}\sum_i \sigma_i \left\{\frac{1}{\varepsilon'(\omega_{i,+})} - \frac{1}{\varepsilon'(\omega_{i,-})}\right\}, \tag{35}$$

with $\sigma_1,\sigma_2 = -1$, $\sigma_3 = 2$. Here the *a priori* noncancellation of the term in brackets was emphasized by Fröhlich as involving long-range $1/r^3$ interactions between the dipoles even when the system is in thermal equilibrium. However, this form of $U(r)$ arises simply as the implicitness has not been solved yet. By using the *Lagrange inversion theorem* [we substitute g of Eq. (B10) with $1/\varepsilon'$ and report the formula in Eq. (35)], one gets immediately that the term in brackets in Eq. (35) vanishes at first order. Expansion of the Lagrange theorem to second order shows that this term goes as $1/r^3$, making U proportional to $1/r^6$, i.e., a short-range contribution. Fröhlich's statement on the existence of *long-range* resonant interactions even at thermal equilibrium is thus *incorrect*. To compute the complete form of U in thermal equilibrium, one can start from Eq. (34) and use the *explicit*

form of $\omega_{i,\pm}(r)$ derived in Appendix B [Eq. (B9)]:

$$U(r) = k_B T \sum_i \ln\left[\left(1 + \frac{\sqrt{\zeta_A\zeta_B}}{2\omega_0^2}\chi'_{ii}(r,\omega_0) + \frac{\zeta_A\zeta_B}{\omega_0}\frac{d}{d\omega}\left[\left(\frac{\chi'_{ii}(r,\omega_0)}{\omega+\omega_0}\right)^2\right]_{\omega_0}\right)\right.$$
$$\left.\times\left(1 - \frac{\sqrt{\zeta_A\zeta_B}}{2\omega_0^2}\chi'_{ii}(r,\omega_0) + \frac{\zeta_A\zeta_B}{\omega_0}\frac{\partial}{\partial\omega}\left[\left(\frac{\chi'_{ii}(r,\omega_0)}{\omega+\omega_0}\right)^2\right]_{\omega_0}\right)\right]$$
$$= k_B T \sum_i \ln\left[1 - \frac{\zeta_A\zeta_B}{4\omega_0^4}(\chi'_{ii}(r,\omega_0))^2 + \frac{\zeta_A\zeta_B}{\omega_0}\left(\frac{\partial\chi'_{ii}(r,\omega_0)}{\partial\omega}\frac{\chi'_{ii}(r,\omega_0)}{2\omega_0^2} - \frac{(\chi'_{ii}(r,\omega_0))^2}{4\omega_0^3}\right)\right].$$

Using the relation $\ln(1+x) \sim x$ valid at large r, the interaction potential becomes

$$U(r) \simeq \frac{k_B T}{2\omega_0^4}\zeta_A\zeta_B\sum_i\left(\omega_0\frac{\partial\chi'_{ii}(r,\omega_0)}{\partial\omega}\chi'_{ii}(r,\omega_0) - (\chi'_{ii}(r,\omega_0))^2\right).$$

In particular, in the limit $r \ll c/\omega_0$, we have from Eqs. (4)

$$\chi'_{ii}(r,\omega_0) = \frac{\sigma_i}{\varepsilon'(\omega_0)r^3}\frac{\partial\chi'_{ii}(r,\omega_0)}{\partial\omega} = \frac{\sigma_i}{r^3}\left(-\frac{1}{[\varepsilon'(\omega_0)]^2}\frac{d\varepsilon'(\omega_0)}{d\omega_0}\right)$$

with $\sigma_1, \sigma_2 = -1, \sigma_3 = 2$. The interaction potential $U(r)$ reads as

$$U(r) = -\frac{3k_B T\zeta_A\zeta_B}{\omega_0^4[\varepsilon'(\omega_0)]^2}\frac{1}{r^6}\left\{1 + \omega_0\frac{d\ln[\varepsilon'(\omega_0)]}{d\omega_0}\right\}. \quad (36)$$

Here, the short-range nature of the potential is due to the use of the Boltzmann distribution which equally weights the normal mode energies. The cancellation of equal long-range contributions with opposite sign [see Eq. (12)] follows. Despite resonance, we conclude that electrodynamic interactions would have negligible effects with respect to Brownian motion, so that electrodynamic interactions at thermal equilibrium are not expected to play a significant role in the dynamics of biomolecules.

VI. EXPERIMENTAL TESTS

As we have shown throughout the present work, from the first principles of electromagnetism we can deduce the existence of electrodynamic interactions among biomolecules due to the vibrations of their electric dipole moments. However, we have also seen that this raises some important questions: (i) Are these electrodynamic interactions sufficiently intense to have any possible biological relevance? (ii) Are the different attenuation mechanisms always so strong as to necessarily suppress even intense electrodynamic interactions? In the end, reliable answers to these questions will be obtained by specific experimental tests. Notice that, following Fröhlich, in order to excite sizable electrodynamic intermolecular forces the excitation of collective molecular vibrations is needed to bring about large vibrating dipole moments, and, moreover, this can affect the biochemical reaction rates [9]. Thus, in two recent papers [5,18] we have suggested how to test the theory given in the present work by means of *in vitro* experiments. Our proposal is to study how the diffusion properties of biomolecules in electrolytic solution vary as a function of the mean intermolecular distance (concentration) once one has excited their collective vibrations. The numerical simulations reported in Ref. [18] have been worked out for physical parameters typical of biomolecules like proteins or small fragments of nucleic acids and have shown a sharp transitional phenomenon occurring at some critical (model dependent) concentration. It has been found that this transition happens at length, time, and concentration scales that allow the application of several available experimental techniques like forced Rayleigh scattering (FRS), fluorescence recovery after photobleaching (FRAP), and fluorescence correlation spectroscopy (FCS), to mention only a few. These kinds of experiments could be performed by using identical molecules, or the cognate partners of some ligand-receptor (protein-protein) or DNA-protein interactions. In any case a crucial point is to be able to excite some out-of-equilibrium collective vibration of the biomolecules under investigation. In fact, as we have shown in the present paper, and contrary to previous predictions [73], electrodynamic interactions are not compatible with thermal equilibrium. The lack of clarity on this point has most probably been the reason why the long-range electrodynamic forces we are after have hitherto eluded observation in spite of many studies on the diffusion behavior of biomolecules in solution. An independent and complementary experimental test would consist in verifying the activation of out-of-equilibrium collective vibrations through spectroscopic techniques. These collective excitations are expected, as already recalled in the Introduction, in the 10^{11}–10^{12}-Hz frequency domain; this domain is nowadays better accessible thanks to new terahertz sources available [59]. In conclusion, an experimental proof of concept would be obtained if, under ascertained out-of-equilibrium collective excitation of some given biomolecules (obtained, for example, by external energy pumping), the above mentioned transitional phenomenon for the diffusion coefficient would be observed. A more complex and still wide open question is how to check the theory in some relevant biological setup. However, there are already some interesting possibilities available. For instance, in [74] the authors show a blue-light-induced dimerization of proteins arabidopsis CIB1 and cryptochrome 2 (CRY2), and have tested the CIB1-CRY2 interaction in mammalian cells finding that after an initial pulse of blue light a mutated version of CRY2 *"rapidly translocated to the plasma membrane."* The authors reported also the ability of the CRY-CIB modules to induce activation of transcription and of DNA recombination. These kind of *in vivo* experiments, together with *in vitro* diffusion experiments performed on the same molecules, are examples of prospective candidates to test the possible biological relevance of the matter discussed in the present work.

VII. CONCLUDING REMARKS

In this paper, long-range electrodynamic interactions (EDIs) between molecular systems have been investigated within a classical framework. Our prime motivation concerns biomolecular dynamics in a cellular environment. Potential functions, i.e., force fields, used in standard molecular dynamics software packages [75,76] usually involve short-distance two-body interaction potentials—i.e., which have minimum influence beyond the Debye length—including screened electrostatic Coulomb forces whose short-range nature is explained by the large amount of ionic entities located in the cell. However, Debye screening only applies for static charges as it becomes inefficient when electric fields with large enough frequency are involved, as was shown by Oro [2]. Since proteins and DNA and RNA molecules are characterized by high-frequency vibrational motions in the terahertz domain or above [14], it is worth investigating how forces of electrodynamic nature may influence the dynamics of biomolecules, especially over long distances. EDIs are well known in QED whereas almost no literature is available on classical interactions. In this paper, we reported that classical EDIs show similar properties as quantum interactions in the dipole limit, i.e., at distances much larger than the dimensions of the molecules involved. Whenever the dipole moments of the molecules oscillate with the same frequency, long-range resonance interactions proportional to $1/r^3$ are activated. Nonresonant conditions lead to short-range interactions proportional to $1/r^6$. Numerical estimates regarding resonance and off-resonance EDIs, e.g., the normal frequency shifts or the equivalent dipoles, were provided in Sec. III. The dipole moments needed to overcome thermal noise at large distance could appear large compared to dipole moments of small standard proteins. However, as suggested by several authors, water ordering of the hydration layers around proteins is expected to lead to more realistic values of their effective dipole moments, whence stronger dipole oscillations and enhanced resonant EDIs occur. Then, despite damping mechanisms prevailing in a biological environment, we have shown that a domain of physical parameters exists for which electrodynamic interactions could be temporarily sustained; this suggests that EDIs could be involved at some stage of biomolecular dynamical organization. In Sec. IV, comparison between classical and quantum EDIs was made. In Sec. V, we emphasize why resonant interactions between biomolecules need nonequilibrium to be effective at a long distance, i.e., the excitation of one normal mode of the interacting system should be statistically "favored" (far beyond Boltzmann fluctuations) compared with other(s) modes. The same conclusion was reached by Tuszynski *et al.* [77] from numerical estimates. In Sec. II, normal modes have been computed from equations of motion (1) omitting anharmonic contributions, dissipative effects, as well as possible external excitations of the oscillating dipoles. Dipole anharmonicities would give rise to nonlinear interactions in normal coordinates. In this case, one might expect long-lived nonequilibrium states lacking energy equipartition among normal modes as, for example, in the case of nonlinearly coupled harmonic oscillators [78]. If so, in a biological context, metabolic energy supply could be of utmost importance to maintain a high degree of excitation in a specific mode despite energy losses. This scenario was originally suggested by Fröhlich [79] who proposed a dynamical model to account for such nonthermal excitations in biological systems. In particular, he showed that a set of coupled normal modes can undergo a condensation phenomenon characterized by the emerging of the mode of *lowest* frequency containing, on the average, nearly all the energy supply [79]. In the case of two interacting molecules, such a process could ensure the action constant of the lowest frequency mode to be much greater than the action constant(s) related to other mode(s). Of course, this would result in an effective attractive potential whose amplitude is dependent on the "stored" energy. Finally, it is worth noting that retardation effects at large r bring about interactions with a $1/r$ dependence [last terms in Eqs. (4)], i.e., of much longer range with respect to the interactions proposed by Fröhlich. This last result could be relevant for a deeper understanding of the highly organized molecular machinery in living matter, as emphasized in the Introduction and in Sec. VI.

ACKNOWLEDGMENT

This work was supported by the Seventh Framework Programme for Research of the European Commission under FET-Open grant TOPDRIM (Grant No. FP7-ICT-318121).

APPENDIX A: ELECTROMAGNETIC FIELD GENERATED BY A TIME-VARYING SOURCE IN A MEDIUM

For the sake of clarity we outline below how the derivation proceeds of Eqs. (4). The starting point is the D'Alembert wave equation for the vector potential $\boldsymbol{A}$ in Fourier space (in Lorenz gauge):

$$\left[k^2 - \frac{\omega^2}{c^2}\varepsilon(\omega)\right]\boldsymbol{A}(\boldsymbol{k},\omega) = \frac{4\pi}{c}\boldsymbol{J}(\boldsymbol{k},\omega). \tag{A1}$$

Here, the dielectric constant $\varepsilon(\omega)$ is simply due to the constitutive relation linking the displacement field $\boldsymbol{D}$ and the macroscopic electric field $\boldsymbol{E}$ in a homogeneous isotropic dielectric medium: $\boldsymbol{D}(\boldsymbol{k},\omega) = \varepsilon(\omega)\boldsymbol{E}(\boldsymbol{k},\omega)$. From Eq. (A1), $\boldsymbol{A}(\boldsymbol{r},\omega)$ can be computed by inverse Fourier transform:

$$\boldsymbol{A}(\boldsymbol{r},\omega) = \frac{4\pi}{c}\left[\frac{1}{(2\pi)^3}\int d^3\boldsymbol{k}\frac{\boldsymbol{J}(\boldsymbol{k},\omega)}{k^2 - \omega^2\varepsilon(\omega)/c^2}e^{i\boldsymbol{k}\cdot\boldsymbol{r}}\right],$$

and by convoluting with the inverse Fourier transform of $\boldsymbol{J}$ we get

$$\boldsymbol{A}(\boldsymbol{r},\omega) = \frac{4\pi}{c}\int d^3\boldsymbol{r}'\left[\frac{1}{(2\pi)^3}\int d^3\boldsymbol{k}\frac{e^{i\boldsymbol{k}\cdot(\boldsymbol{r}-\boldsymbol{r}')}}{k^2 - \omega^2\varepsilon(\omega)/c^2}\right] \times \boldsymbol{J}(\boldsymbol{r}',\omega). \tag{A2}$$

The kernel is computed using spherical coordinates and integrating over the angles:

$$\begin{aligned} I(\boldsymbol{r},\omega) &\equiv \frac{1}{(2\pi)^3}\int d^3\boldsymbol{k}\frac{e^{i\boldsymbol{k}\cdot\boldsymbol{r}}}{k^2 - \omega^2\varepsilon(\omega)/c^2} \\ &= \frac{1}{(2\pi)^3}\int_0^\infty k^2 dk\int_0^\pi \sin(\theta)d\theta \\ &\quad\times\int_0^{2\pi} d\varphi\frac{e^{ik\cos(\theta)r}}{k^2 - \omega^2\varepsilon(\omega)/c^2}, \end{aligned}$$

where, without loss of generality, the z axis of the Cartesian coordinate system has been taken along $\boldsymbol{r}$, so that $\boldsymbol{k}\cdot\boldsymbol{r} = k\cos(\theta)r$. We show that $I(\boldsymbol{r},\omega)$ satisfy

$$I(\boldsymbol{r},\omega) = \frac{-i}{(2\pi)^2 r}\int_0^\infty dk \frac{k}{k^2-\omega^2\varepsilon(\omega)/c^2}[e^{ikr}-e^{-ikr}].$$

In order to use the residue theorem, k is substituted with $-k$ in the second term of the integrand to give

$$I(\boldsymbol{r},\omega) = \frac{-i}{(2\pi)^2 r}\int_{-\infty}^\infty dk \frac{k}{k^2-\omega^2\varepsilon(\omega)/c^2}e^{ikr}.$$

Then the function

$$f(z) = ze^{izr}\left(z^2-\frac{\omega^2}{c^2}\varepsilon(\omega)\right)^{-1},$$

is integrated on the semicircular contour of the upper complex plane which includes the real axis. In this case, $|zf(z)|$ approaches zero as $|z|$ approaches $+\infty$. Of the two simple poles of f at $z = \pm z_0 = \pm\omega\sqrt{\varepsilon(\omega)}/c$ only one of them is located inside the contour. When $\mathrm{Im}(\omega\sqrt{\varepsilon(\omega)}) > 0$, the pole will be $+z_0$, and vice versa. Hence, I is simply found to be

$$I(\boldsymbol{r},\omega) = \frac{1}{4\pi r}e^{\pm i\omega\sqrt{\varepsilon(\omega)}r/c}, \tag{A3}$$

when $\mathrm{Im}(\omega\sqrt{\varepsilon(\omega)})$ is positive or negative, respectively, and Eq. (A2) yields

$$\boldsymbol{A}(\boldsymbol{r},\omega) = \frac{1}{c}\int d^3\boldsymbol{r}'\frac{e^{\pm i\omega\sqrt{\varepsilon(\omega)}||\boldsymbol{r}-\boldsymbol{r}'||/c}}{||\boldsymbol{r}-\boldsymbol{r}'||}\boldsymbol{J}(\boldsymbol{r}',\omega). \tag{A4}$$

Assuming the current $\boldsymbol{J}(\boldsymbol{r}',\omega)$ is due to a molecule whose center of mass is far from where the field is measured, one can take $r \gg r'$ and $||\boldsymbol{r}-\boldsymbol{r}'||$ can be approximated as

$$||\boldsymbol{r}-\boldsymbol{r}'|| = r\sqrt{1-\frac{2\,\boldsymbol{r}'\cdot\boldsymbol{r}}{r^2}+\left(\frac{r'}{r}\right)^2} \simeq r-\boldsymbol{r}'\cdot\boldsymbol{n}+\cdots$$

where we have let $\boldsymbol{n}\equiv\boldsymbol{r}/r$. Thus

$$e^{\pm i\omega\sqrt{\varepsilon(\omega)}||\boldsymbol{r}-\boldsymbol{r}'||/c} \simeq e^{\pm i\omega\sqrt{\varepsilon(\omega)}r/c}\left(1\mp\frac{i\omega\sqrt{\varepsilon(\omega)}}{c}\,\boldsymbol{r}'\cdot\boldsymbol{n}+\cdots\right). \tag{A5}$$

Likewise, one has

$$\frac{1}{||\boldsymbol{r}-\boldsymbol{r}'||} = \frac{1}{r}\left(1-\frac{2\,\boldsymbol{r}'\cdot\boldsymbol{r}}{r^2}+\left(\frac{r'}{r}\right)^2\right)^{-1/2} \simeq \frac{1}{r}(1+\boldsymbol{r}'\cdot\boldsymbol{n}+\cdots). \tag{A6}$$

1. Dipole approximation

Considering only the first terms of the expansion in Eqs. (A5) and (A6), as a first approximation, one gets

$$\boldsymbol{A}(\boldsymbol{r},\omega) \simeq \frac{e^{\pm i\omega\sqrt{\varepsilon(\omega)}r/c}}{cr}\int d^3\boldsymbol{r}'\,\boldsymbol{J}(\boldsymbol{r}',\omega) \simeq -\frac{e^{\pm i\omega\sqrt{\varepsilon(\omega)}r/c}}{cr}\int d^3\boldsymbol{r}'\,\boldsymbol{r}'(\nabla\cdot\boldsymbol{J}(\boldsymbol{r}',\omega)).$$

Making use of the continuity equation, one finds

$$\boldsymbol{A}(\boldsymbol{r},\omega) = -\frac{i\omega}{cr}e^{\pm i\omega\sqrt{\varepsilon(\omega)}r/c}\,\boldsymbol{\mu}(\omega), \tag{A7}$$

where $\boldsymbol{\mu}(\omega) = \int d^3\boldsymbol{r}'\boldsymbol{r}'\rho(\boldsymbol{r}',\omega)$ is the (macroscopic) dipole moment associated with the distribution of charge ρ of a molecule. Using (macroscopic) Maxwell equations $\boldsymbol{B} = \nabla\times\boldsymbol{A}$ and $\nabla\times\boldsymbol{B} = \boldsymbol{J} - i\omega\varepsilon(\omega)\boldsymbol{E}/c$, we can easily find the magnetic and electric components of the radiation field:

$$\boldsymbol{B}(\boldsymbol{r},\omega) = \frac{i\omega\sqrt{\varepsilon(\omega)}}{c}\frac{e^{\pm i\omega\sqrt{\varepsilon(\omega)}r/c}}{r^2}(\boldsymbol{n}\times\boldsymbol{\mu}(\omega)) \times\left(1\mp\frac{i\omega\sqrt{\epsilon(\omega)}r}{c}\right), \tag{A8}$$

$$\boldsymbol{E}(\boldsymbol{r},\omega) = -\frac{ic}{\omega\varepsilon(\omega)}\boldsymbol{J}(\boldsymbol{r},\omega) - \frac{e^{\pm i\omega\sqrt{\varepsilon(\omega)}r/c}}{\varepsilon(\omega)r^3} \times\left\{[\boldsymbol{\mu}(\omega)-3\boldsymbol{n}(\boldsymbol{n}\cdot\boldsymbol{\mu}(\omega))]\left(1\mp\frac{i\omega\sqrt{\varepsilon(\omega)}r}{c}\right)\right. \times\left.-[\boldsymbol{\mu}(\omega)-\boldsymbol{n}(\boldsymbol{n}\cdot\boldsymbol{\mu}(\omega))]\frac{\omega^2\varepsilon(\omega)r^2}{c^2}\right\}. \tag{A9}$$

Again, let us stress that these equations are valid for r large with respect to the size of the molecule. Hence, we can assume $\boldsymbol{J}(\boldsymbol{r},\omega) = 0$ in Eq. (A9) and write the electromagnetic field in the compact form

$$\begin{aligned}\boldsymbol{B}(\boldsymbol{r},\omega) &= \boldsymbol{\chi}^B(r,\omega)\boldsymbol{\mu}(\omega),\\ \boldsymbol{E}(\boldsymbol{r},\omega) &= \boldsymbol{\chi}^E(r,\omega)\boldsymbol{\mu}(\omega),\end{aligned} \tag{A10}$$

where $\boldsymbol{\chi}^B(\boldsymbol{r},\omega)$ and $\boldsymbol{\chi}^E(\boldsymbol{r},\omega)$ are the susceptibility matrix of the magnetic and electric fields. In particular, $\boldsymbol{\chi}^B(\boldsymbol{r},\omega)$ and $\boldsymbol{\chi}^E(\boldsymbol{r},\omega)$ can be given in a diagonal form by taking the z axis along $\boldsymbol{n}$. In this case,

$$\chi^B_{12}(\boldsymbol{r},\omega) = \chi^B_{21}(\boldsymbol{r},\omega) = \frac{i\omega\sqrt{\varepsilon(\omega)}}{c}\frac{e^{\pm i\omega\sqrt{\varepsilon(\omega)}r/c}}{r^2}\left(1\mp\frac{i\omega\sqrt{\epsilon(\omega)}r}{c}\right),$$

$$\text{and}\quad \chi^B_{ij}(\boldsymbol{r},\omega) = 0 \quad \text{elsewhere}, \tag{A11}$$

regarding the magnetic field, and

$$\chi^E_{11}(\boldsymbol{r},\omega) = \chi^E_{22}(\boldsymbol{r},\omega) = -\frac{e^{\pm i\omega\sqrt{\varepsilon(\omega)}r/c}}{\varepsilon(\omega)r^3} \times\left(1\mp\frac{i\omega\sqrt{\varepsilon(\omega)}r}{c}-\frac{\omega^2\varepsilon(\omega)r^2}{c^2}\right),$$

$$\chi^E_{33}(\boldsymbol{r},\omega) = \frac{2e^{\pm i\omega\sqrt{\varepsilon(\omega)}r/c}}{\varepsilon(\omega)r^3}\left(1\mp\frac{i\omega\sqrt{\varepsilon(\omega)}r}{c}\right),\ \text{and}$$

$$\chi^E_{ij}(\boldsymbol{r},\omega) = 0 \quad \text{for } i\neq j, \tag{A12}$$

regarding the electric field.

Equation (A12) is the same as Eq. (4) of Sec. II where we considered two harmonic dipoles A and B, so that $\boldsymbol{\mu}$ in Eq. (A10) should be replaced by $\boldsymbol{\mu}(\omega) = \boldsymbol{\mu}_{A,B}\delta(\omega-\omega_N)$.

APPENDIX B: USE OF COMPLEX ANALYSIS TO ESTIMATE OFF-RESONANCE AND RESONANT FREQUENCY SHIFTS

1. Off-resonance case

To find explicit solutions of Eq. (7), we apply the Lagrange inversion theorem of complex analysis which states the following [80]:

Let $\mathscr{C}$ be a contour in the complex plane, and let f a function analytic inside, and on $\mathscr{C}$. Let Θ be another function which is analytic inside it and on $\mathscr{C}$ except at a finite number of poles. Noting $a_1,\ldots,a_n$ the zeros of f in the interior of $\mathscr{C}$, of degree of multiplicity $r_1,\ldots r_n$, and $b_1,\ldots,b_m$ the poles of f of degree of multiplicity $s_1,\ldots,s_m$, one has the following formula:

$$\sum_{j=1}^{n} r_j f(a_j) - \sum_{k=1}^{m} s_k f(b_k) = \frac{1}{2i\pi}\oint_{\mathscr{C}} dz f(z)\partial_z \ln\Theta(z). \tag{B1}$$

In the present context, if $\mathscr{C}$ is a contour on and inside which $\Theta_{i,\pm}$ is analytic, and that contains only one solution $\omega_{i,\pm}(r)$ of Eq. (7), f can be taken as the identity function and Θ as $\Theta_{i,\pm}(r,\omega)$, so that

$$\omega_{i,\pm}(r) = \frac{1}{2i\pi}\oint_{\mathscr{C}} dz\; z\; \partial_z \ln\Theta_{i,\pm}(r,z). \tag{B2}$$

Now, regarding the contour, we choose $\mathscr{C}$ on the right part of the complex plane (complex numbers with positive real values) and we suppose that the inequality

$$\frac{\zeta_A\zeta_B(\chi'_{ii}(r,z))^2}{\omega_A^2-\omega_B^2} < \left|z^2-\omega_{A,B}^2\right| \tag{B3}$$

holds for all z on the perimeter of $\mathscr{C}$. On the other hand, since each χ'_{ii}, $i=1,2,3$, is a sum of inverse power laws of r, we can assume that, for large r, relation (B3) is satisfied. In this case, by applying Rouché's theorem, it is seen that $\omega_{A,B}$ is located inside $\mathscr{C}$. Thus, by inserting Eq. (7) into Eq. (B2), one has

$$\omega_{i,\pm}(r) = \underbrace{\frac{1}{2\pi i}\oint_{\mathscr{C}} dz\; z\; \partial_z \ln\left[z^2-\omega_{A,B}^2\right]}_{\omega_{A,B}} + \frac{1}{2\pi i}\oint_{\mathscr{C}} dz\; z\; \partial_z \times \ln\left[1\mp\frac{\zeta_A\zeta_B(\chi'_{ii}(r,z))^2}{\left(z^2-\omega_{A,B}^2\right)\left(\omega_A^2-\omega_B^2\right)}\right]. \tag{B4}$$

The second integral is computed by integration by parts. After Taylor expansion of the logarithm, one gets

$$\omega_{i,\pm}(r) \simeq \omega_{A,B} \pm \frac{1}{2\pi i}\oint_{\mathscr{C}} dz \frac{\zeta_A\zeta_B(\chi'_{ii}(r,z))^2}{\left(z^2-\omega_{A,B}^2\right)\left(\omega_A^2-\omega_B^2\right)}, \tag{B5}$$

at lowest order. On the other hand, since the function $\zeta_A\zeta_B(\chi'_{ii}(r,z))^2/(z+\omega_{A,B})(\omega_A^2-\omega_B^2)$ is analytic everywhere inside $\mathscr{C}$, we can make use of Cauchy's integral formula to find exactly Eq. (8).

2. Resonance case

Similarly to the nonresonant case, we find that if $\Theta_{i,\pm}(r,z)$ of Eq. (11) is analytical inside and on a contour $\mathscr{C}$ around $\omega_{i,\pm}$, and for which the inequality

$$\sqrt{\zeta_A\zeta_B}\chi'_{ii}(r,z) < \left|z^2-\omega_0^2\right|, \tag{B6}$$

is valid for all z on $\mathscr{C}$, then ω_0 is also located inside the contour and the solution $\omega_{i,\pm}(r)$ may be given by

$$\omega_{i,\pm}(r) = \underbrace{\frac{1}{2\pi i}\oint_{\mathscr{C}} dz\; z\; \partial_z \ln\left[z^2-\omega_0^2\right]}_{\omega_0} - \frac{1}{2\pi i}\oint_{\mathscr{C}} dz \ln\left[1\mp\frac{\sqrt{\zeta_A\zeta_B}\chi'_{ii}(r,z)}{z^2-\omega_0^2}\right]. \tag{B7}$$

In comparison with Eq. (7), Eq. (11) is exact, so it makes sense to write the complete series expansion of the logarithm:

$$\omega_{i,\pm}(r) = \omega_0 + \sum_{n=1}^{\infty}\frac{(\pm1)^n}{2\pi i n}\oint_{\mathscr{C}} dz\left\{\frac{\sqrt{\zeta_A\zeta_B}\chi'_{ii}(r,z)}{z^2-\omega_0^2}\right\}^n = \omega_0 + \sum_{n=1}^{\infty}\frac{(\pm1)^n}{2\pi i n}\oint_{\mathscr{C}} dz\frac{1}{(z-\omega_0)^n}\left\{\frac{\sqrt{\zeta_A\zeta_B}\chi'_{ii}(r,z)}{z+\omega_0}\right\}^n. \tag{B8}$$

Hence, Cauchy's integral formula may be applied at all orders to the function in brackets since it is analytic inside and on $\mathscr{C}$:

$$\omega_{i,\pm}(r) = \omega_0 + \sum_{n=1}^{\infty}\frac{(\pm1)^n}{n!}\frac{d^{n-1}}{d\omega^{n-1}}\left[\left\{\frac{\sqrt{\zeta_A\zeta_B}\chi'_{ii}(r,\omega)}{\omega+\omega_0}\right\}^n\right]_{\omega=\omega_0}. \tag{B9}$$

Using similar arguments, it may be shown that any function f analytic on and inside $\mathscr{C}$ may be expanded as a power series in $\omega_{i,\pm}(r)$ through the formula

$$g(\omega_{i,\pm}(r)) = g(\omega_0) + \sum_{n=1}^{\infty}\frac{(\pm1)^n}{n!}\frac{d^{n-1}}{d\omega^{n-1}}\left[g'(\omega)\left\{\frac{\sqrt{\zeta_A\zeta_B}\chi'_{ii}(r,\omega)}{\omega+\omega_0}\right\}^n\right]_{\omega=\omega_0}. \tag{B10}$$

By considering Eq. (B9) at lowest order, one exactly obtains Eq. (12) of the main text.

[1] S. Zhao and R. Iyengar, Systems pharmacology: Network analysis to identify multiscale mechanisms of drug action, Annu. Rev. Pharmacol. Toxicol. **52**, 505 (2012).

[2] J. R. de Xammar Oro, G. Ruderman, J. R. Grigera, and F. Vericat, Threshold frequency for the ionic screening of electric fields in electrolyte solutions, J. Chem. Soc., Faraday Trans. **88**, 699 (1992); J. R. de Xammar Oro, G. Ruderman, and J. R. Grigera, Electrodynamics of interactions in electrolyte media. Possible consequences in biological functions, Biophysics **53**, 195 (2008).

[3] J. C. Maxwell, *A Treatise on Electricity and Magnetism* (Dover, New York, 1954).

[4] See, for example, M. J. Stephen, First-order dispersion forces, J. Chem. Phys. **40**, 669 (1964); A. D. McLachlan, Resonance transfer of molecular excitation energy, Mol. Phys. **8**, 409 (1964), in the case of two identical atoms; D. P. Craig and T. Thirunamachandran, *Molecular Quantum Electrodynamics* (Academic, London, 1984).

[5] J. Preto, E. Floriani, I. Nardecchia, P. Ferrier, and M. Pettini, Experimental assessment of the contribution of electrodynamic interactions to long-distance recruitment of biomolecular partners: Theoretical basis, Phys. Rev. E **85**, 041904 (2012).

[6] J. Preto, Long-range interactions in biological systems, Ph.D. thesis, Aix-Marseille University, 2012.

[7] I. Nardecchia, Feasibility study of the experimental detection of long-range selective resonant recruitment forces between biomolecules, Ph.D. thesis, Aix-Marseille University, 2012.

[8] H. Fröhlich, Selective long range dispersion forces between large systems, Phys. Lett. A **39**, 153 (1972).

[9] H. Fröhlich, The extraordinary dielectric properties of biological materials and the action of enzymes, Proc. Natl. Acad. Sci. U.S.A. **72**, 4211 (1975).

[10] H. Fröhlich, Coherent electric vibrations in biological systems and the cancer problem, IEEE Trans. Microwave Theory & Tech. **26**, 613 (1978).

[11] H. Fröhlich, The biological effects of microwaves and related questions, Adv. Electron. Electron Phys. **53**, 85 (1980).

[12] J. Preto and M. Pettini, Resonant long-range interactions between polar macromolecules, Phys. Lett. A **377**, 587 (2013).

[13] L. D. Landau and E. M. Lifshitz, *Statistical Physics* (Pergamon Press, New York, 1980).

[14] P. C. Painter, L. E. Mosher, and C. Rhoads, Low-frequency modes in the Raman spectra of proteins, Biopolymers **21**, 1469 (1982); K. C. Chou, Low-frequency motions in protein molecules. Beta-sheet and beta-barrel, Biophys. J. **48**, 289 (1985).

[15] J. B. Hasted, Liquid water: Dielectric properties, in *Water: A Comprehensive Treatise*, edited by F. Franks (Plenum Press, New York, 1972), Vol. 1, pp. 255–309.

[16] M. Cifra, J. Pokorný, D. Havelka, and O. Kučera, Electric field generated by axial longitudinal vibration modes of microtubule, BioSystems **100**, 122 (2010).

[17] F. Jelínek, M. Cifra, J. Pokorný, J. Vaniš, J. Šimša, J. Hašek, and I. Frýdlová, Measurement of electrical oscillations and mechanical vibrations of yeast cells membrane around 1 kHz, Electromagn. Biol. Med. **28**, 223 (2009).

[18] I. Nardecchia, L. Spinelli, J. Preto, M. Gori, E. Floriani, S. Jaeger, P. Ferrier, and M. Pettini, Experimental detection of long-distance interactions between biomolecules through their diffusion behavior: Numerical study, Phys. Rev. E **90**, 022703 (2014).

[19] S. Takashima, Measurement and computation of the dipole moment of globular proteins III: chymotrypsin, Biophys. Chem. **58**, 13 (1996).

[20] S. Takashima, Electric dipole moments of globular proteins: Measurement and calculation with NMR and X-ray databases, J. Non-Cryst. Solids **305**, 303 (2002).

[21] S. R. Kabir, K. Yokoyama, K. Mihashi, T. Kodama, and M. Suzuki, Hyper-mobile water is induced around actin filaments, Biophys. J. **85**, 3154 (2003).

[22] G. H. Pollack, *The Fourth Phase of Water: Beyond Solid, Liquid, and Vapor* (Ebner & Sons, Seattle, 2013).

[23] G. M. Giambasu, T. Luchko, D. Herschlag, D. M. York, and D. A. Case, Ion counting from explicit-solvent simulations and 3D-RISM, Biophys. J. **106**, 883 (2014).

[24] J. A. Tuszyński, E. J. Carpenter, J. M. Dixon, and Y. Engelborghs, Non-Gaussian statistics of the vibrational fluctuations of myoglobin, Eur. Biophys. J. **33**, 159 (2004).

[25] A. Ben-Naim, *Water and Aqueous Solutions* (Plenum, New York, 1974).

[26] J. A. Tuszyński, J. A. Brown, E. Crawford, E. J. Carpenter, M. L. A. Nip, J. M. Dixon, and M. V. Satarić, Molecular dynamics simulations of tubulin structure and calculations of electrostatic properties of microtubules, Math. Comput. Model. **41**, 1055 (2005).

[27] J. D. Jackson, *Classical Electrodynamics*, 6th printing (John Wiley & Sons, Inc., New York, 1967).

[28] W. K. H. Panofsky and M. Phillips, *Classical Electricity and Magnetism* (Addison-Wesley, New York, 1962).

[29] B. Alberts, A. Johnson, J. Lewis, M. Raff, K. Roberts, and P. Walter, *Molecular Biology of the Cell*, 2nd ed. (Garland Publishing, Inc., New York, 1989), pp. 93–94, pp. 354–355.

[30] P. Debye, Reaction rates in ionic solutions, Trans. Electrochem. Soc. **82**, 265 (1942).

[31] R. M. Noyes, Effects of diffusion rates on chemical kinetics in *Progress in Reaction Kinetics*, Vol. 1, edited by G. Porter (Pergamon Press, New York, 1961), p. 128.

[32] J. Howard, *Mechanics of Motor Proteins and the Cytoskeleton* (Sinauer Associates, Inc., Sunderland, 2001), pp. 41–45.

[33] J. J. Chang, Physical properties of biophotons and their biological functions, Indian J. Exp. Biol. **46**, 371 (2008).

[34] S. Cohen and F. A. Popp, Biophoton emission of the human body, J. Photochem. Photobiol. B **40**, 187 (1997).

[35] B. Devaraj, R. Q. Scott, P. Roschger, and H. Inaba, Ultraweak light emission from rat liver nuclei, Photochem. Photobiol. **54**, 289 (1991).

[36] M. Kobayashi, D. Kikuchi, and H. Okamura, Imaging of ultraweak spontaneous photon emission from human body displaying diurnal rhythm, PLoS One **4**, e6256 (2009).

[37] M. Kobayashi, M. Takeda, K.-I. Ito, H. Kato, and H. Inaba, Two-dimensional photon counting imaging and spatiotemporal characterization of ultraweak photon emission from a rat's brain in vivo, J. Neurosci. Methods **93**, 163 (1999).

[38] T. I. Quickenden and S. S. Que Hee, Weak luminescence from the yeast saccharomyces cerevisiae and the existence of mitogenetic radiation, Biochem. Biophys. Res. Commun. **60**, 764 (1974).

[39] M. Takeda, M. Kobayashi, M. Takayama, S. Suzuki, T. Ishida, K. Ohnuki, T. Moriya, and N. Ohuchi, Biophoton detection

as a novel technique for cancer imaging, Cancer Sci. **95**, 656 (2004).

[40] R. van Wijk, J. M. Ackerman, and E. P. van Wijk, Effects of a color filter used in auriculomedicine on ultraweak photon emission of the human body, J. Altern. Complement. Med. **12**, 955 (2006).

[41] Y. Z. Yoon, J. Kim, B. C. Lee, Y. U. Kim, S. K. Lee, and K. S. Soh, Changes in ultraweak photon emission and heart rate variability of epinephrine-injected rats, Gen. Physiol. Biophys. **24**, 147 (2005).

[42] R. Thar and M. Kuhl, Propagation of electromagnetic radiation in mitochondria? J. Theor. Biol. **230**, 261 (2004).

[43] M. Nakano, Low-level chemiluminescence during lipid peroxidations and enzymatic reactions, J. Biolumin. Chemilum. **4**, 231 (2005).

[44] Y. Isojima, T. Isoshima, K. Nagai, K. Kikuchi, and H. Nakagawa, Ultraweak biochemiluminescence detected from rat hippocampal slices, Neuro. Rep. **6**, 658 (1995).

[45] Y. Kataoka, Y. Cui, A. Yamagata, M. Niigaki, T. Hirohata, N. Oishi, and Y. Watanabe, Activity-dependent neural tissue oxidation emits intrinsic ultraweak photons, Biochem. Biophys. Res. Commun. **285**, 1007 (2001).

[46] M. Kobayashi, M. Takeda, T. Sato, Y. Yamazaki, K. Kaneko, K. I. Ito, H. Kato, and H. Inaba, In vivo imaging of spontaneous ultraweak photon emission from a rats brain correlated with cerebral energy metabolism and oxidative stress, Neurosci. Res. **34**, 103 (1999).

[47] Y. Sun, C. H. Wang, and J. Dai, Biophotons as neural communication signals demonstrated by *in situ* biophoton autography, Photochem. Photobiol. Sci. **9**, 315 (2010).

[48] V. Voeikov, Reactive oxygen species, water, photons and life, Rivista di Biologia/Biology Forum **94**, 237 (2001).

[49] J. T. Kindt and C. A. Schmuttenmaer, Far-infrared dielectric properties of polar liquids probed by femtosecond terahertz pulse spectroscopy, J. Phys. Chem. **100**, 10373 (1996).

[50] J. B. Hasted, S. K. Husain, F. A. M. Frescura, and J. R. Birch, Far-infrared absorption in liquid water, Chem. Phys. Lett. **118**, 622 (1985).

[51] G. J. Wilmink, B. D. Rivest, B. L. Ibey, L. X. Cundin, E. C. Haywood, and W. P. Roach, The optical properties of biological tissues in the terahertz wavelength range, Proc. SPIE **7175**, 717507 (2009).

[52] C. T. Tai and R. E. Collin, Radiation of a Hertzian dipole immersed in a dissipative medium, IEEE Trans. Antennas Propag. **48**, 1501 (2000).

[53] K. G. Brown, S. C. Erfurth, E. W. Small, and W. L. Peticolas, Conformationally dependent low-frequency motions of proteins by laser Raman spectroscopy, Proc. Natl. Acad. Sci. U.S.A. **69**, 1467 (1972).

[54] L. Genzel, F. Keilmann, T. P. Martin, G. Wintreling, Y. Yacoby, H. Fröhlich, and M. W. Makinen, Low-frequency Raman spectra of lysozyme, Biopolymers **15**, 219 (1976).

[55] H. Urabe, Y. Sugawara, M. Ataka, and A. Rupprecht, Low-frequency Raman spectra of lysozyme crystals and oriented DNA films: Dynamics of crystal water, Biophys. J. **74**, 1533 (1998).

[56] Y. M. Romanovsky, A. V. Netrebko, and A. Y. Chikishev, Are the subglobular oscillations of protein molecules in water overdamped?, in Saratov Fall Meeting 2001 (International Society for Optics and Photonics): Optical Technologies in Biophysics and Medicine III, pp. 16–29 (2002).

[57] K. R. Foster and J. W. Baish, Viscous damping of vibrations in microtubules, J. Biol. Phys. **26**, 255 (2000).

[58] R. K. Adair, Vibrational resonances in biological systems at microwave frequencies, Biophys. J. **82**, 1147 (2002).

[59] V. Conti Nibali and M. Havenith, New insights into the role of water in biological function: Studying solvated biomolecules using terahertz absorption spectroscopy in conjunction with molecular dynamics simulations, J. Am. Chem. Soc. **136**, 12800 (2014).

[60] J. Pokorný, Excitation of vibrations in microtubules in living cells, Bioelectrochemistry **63**, 321 (2004).

[61] G. S. Edwards, C. C. Davis, J. D. Saffer, and M. L. Swicord, Resonant microwave absorption of selected DNA molecules, Phys. Rev. Lett. **53**, 1284 (1984).

[62] L. L. Van Zandt, Resonant microwave absorption by dissolved DNA, Phys. Rev. Lett. **57**, 2085 (1986).

[63] L. L. Van Zandt, Why structured water causes sharp absorption by DNA at microwave frequencies, J. Biomol. Struct. Dyn. **4**, 569 (1987).

[64] F. Gruia, M. Kubo, X. Ye, and P. M. Champion, Investigations of vibrational coherence in the low-frequency region of ferric heme proteins, Biophys. J. **94**, 2252 (2008).

[65] T. Cimei, A. R. Bizzarri, S. Cannistraro, G. Cerullo, and S. De Silvestri, Vibrational coherence in Azurin with impulsive excitation of the LMCT absorption band, Chem. Phys. Lett. **362**, 497 (2002).

[66] D. A. Turton, H. M. Senn, T. Harwood, A. J. Lapthorn, E. M. Ellis, and K. Wynne, Terahertz underdamped vibrational motion governs protein-ligand binding in solution, Nat. Commun. **5**, 3999 (2014).

[67] A. Xie, A. F. G. van der Meer, and R. H. Austin, Excited-state lifetimes of far-infrared collective modes in proteins, Phys. Rev. Lett. **88**, 018102 (2001).

[68] V. V. Mitrofanov, Y. M. Romanovsky, and A. V. Netrebko, On the structure and dynamics of hydrogen bonds in liquid water, in Saratov Fall Meeting 2003 (International Society for Optics and Photonics): Optical Technologies in Biophysics and Medicine V, pp. 42-48 (2004).

[69] L. Gomberoff, R. R. McLone, and E. A. Power, Long-range retarded potentials between molecules, J. Chem. Phys. **44**, 4148 (1966).

[70] R. R. McLone and E. A. Power, The long range van der Waals forces between non-identical systems, Proc. R. Soc. London, Ser. A **286**, 573 (1965); G.-I. Kweon and N. M. Lawandy, Dispersion interactions between excited atoms, Phys. Rev. A **47**, 4513 (1993); Erratum: Dispersion interactions between excited atoms, *ibid.* **49**, 2205 (1994).

[71] E. A. Power and T. Thirunamachandran, Casimir-Polder potential as an interaction between induced dipoles, Phys. Rev. A **48**, 4761 (1993).

[72] H. B. G. Casimir and D. Polder, The influence of retardation on the London-van der Waals forces, Phys. Rev. **73**, 360 (1948).

[73] H. Fröhlich, Long-range coherence in biological systems, Riv. Nuovo Cimento **7**, 399 (1977).

[74] M. J. Kennedy, R. M. Hughes, L. A. Peteya, J. W. Schwartz, M. D. Ehlers, and C. L. Tucker, Rapid blue-light-mediated

induction of protein interactions in living cells, Nat. Methods **7**, 973 (2010).

[75] D. Van Der Spoel, E. Lindahl, B. Hess, G. Groenhof, A. E. Mark, and H. J. C. Berendsen, GROMACS: fast, flexible, and free, J. Comput. Chem. **26**, 1701 (2005).

[76] D. A. Pearlman, D. A. Case, J. W. Caldwell, W. S. Ross, T. E. Cheatham, S. DeBolt, D. Ferguson, G. Seibel, and P. Kollman, AMBER, a package of computer programs for applying molecular mechanics, normal mode analysis, molecular dynamics and free energy calculations to simulate the structural and energetic properties of molecules, Comput. Phys. Commun. **91**, 1 (1995).

[77] J. A. Tuszyński and E. K. Strong, Application of the Fröhlich theory to the modelling of rouleau formation in human erythrocytes, J. Biol. Phys. **17**, 19 (1989).

[78] M. Pettini, *Geometry and Topology in Hamiltonian Dynamics and Statistical Mechanics* (Springer, New York, 2007).

[79] H. Fröhlich, Long-range coherence and energy storage in biological systems, Int. J. Quantum Chem. **2**, 641 (1968).

[80] E. T. Whittaker and G. N. Watson, *A Course of Modern Analysis*, 4th ed. (Cambridge University Press, Cambridge, England, 1927), pp. 131–133.